Absolute asymmetric synthesis from an isotropic racemic mixture of chiral molecules with the help of their laser orientation-dependent selection

Dmitry V. Zhdanov[a] and Victor N. Zadkov[b]
International Laser Center and Faculty of Physics, M. V. Lomonosov Moscow State University, 119992 Moscow, Russia

(Received 17 September 2007; accepted 1 October 2007; published online 28 December 2007)

We analyzed the absolute asymmetric synthesis (AAS) of enantiomers from an isotropic racemic mixture of chiral molecules, which employs the laser electrodipole interaction, and revealed a set of basic symmetry-based conditions on the parameters of field-molecule interaction. Using these conditions, we developed a novel scenario of the AAS (through selective photodestruction of the enantiomers of a given type) based on the joint action of the strong multicomponent femtosecond and picosecond laser pulses. Key mechanism of this scenario is the partly modified scheme of laser orientation-dependent selection of molecules proposed by us earlier [D. V. Zhdanov *et al.*, JETP **130**, 387 (2006)]. Calculations made on example of chiral molecule SiHNaClF show rather high efficiency and stability of the proposed AAS scenario with respect to the parameters of the incident laser pulses and even feasibility of its realization at room temperature. © *2007 American Institute of Physics*. [DOI: 10.1063/1.2801640]

I. INTRODUCTION

The property of any asymmetric molecule to exist in the form of two isomers or so called left- (*L*) and right-handed (*D*) enantiomers, which are the mirror images of each other, is called *molecular chirality*. The *L* and *D* enantiomers would have different physical-chemical and biological properties: for instance, smell differently, have different toxicity, pharmacological activity, etc. Therefore, the absolute asymmetric synthesis (AAS) of a required enantiomer from a racemic mixture (i.e., a mixture that contains 50 to 50% of different enantiomers) is not only a challenging problem for many decades for physicists but is also of great importance for various problems in chemistry and pharmaceutical industry. Key difficulty here is that both enantiomers have absolutely identical scalar physical properties, which does not allow a trivial solution for the AAS. In chemistry, this obstacle can be overcome if one uses the pure chiral chemical reagents, but this raises then a problem of synthesis of such pure chiral reagents themselves. At the same time, chemical synthesis of a racemic mixture of chiral molecules is in some cases a routine task. Therefore, along with the development of the chemical methods, which use pure chiral reagents, investigation of AAS feasibility from a racemic mixture seems to be very perspective and is considered in this paper.

In the last decade, it has been demonstrated that the methods of laser physics and specifically the methods of coherent control are universal and extremely effective tools for controlling molecular dynamics.[1] One can suppose then that they can also be effectively applied for the solution of the AAS problem.[2] Theoretically, laser-assisted AAS has been intensively studied in the literature. Various ways of laser field-molecule interactions were analyzed: electric quadrupole and magnitochiral (see Refs. 3 and 4 and references therein), joint electro- and magnetodipole,[5–7] and pure electrodipole interactions.[8–32] However, despite all these theoretical studies and variety of developed scenarios, only two ways of enantiomeric enrichment have been demonstrated experimentally. The first one is based on the electroquarupole interaction with circularly polarized light[33–36] and the second one is based on the interaction with the laser field in the presence of a strong dc magnetic field (magnetochiral effect).[37] Unfortunately, such interactions, as well as the magnetodipole interactions, are ineffective for small chiral molecules.[38] This is because electroquadrupole, magnetochiral, and magnetodipole effects in such molecules are very weak and, as a rule, are suppressed by the dominated electrodipole interaction. Therefore, the latter is widely analyzed in the bulk of available literature.

The question arises then why none of the laser-assisted AAS scenarios suggested in Refs. 8–32 has been realized experimentally. Surely, one of the obstacle for this is that it is difficult to detect the results of the AAS as in most cases enantiomers of the molecules under consideration spontaneously interconverted at the short time of about 10^{-9}–10^{-11} s (the case of so called unstable or dynamical chirality).

Even more essential difficulty for experimental realization of the scenarios suggested in Refs. 8–21 is that the molecules must be preliminary oriented in space in a way that at least one of their molecule-fixed axes must be codirected with the space-fixed direction. Note that nowadays only those laser techniques are rather well developed, which lead to collinear (but not necessarily parallel) alignment of the molecule-fixed axes (see, for example, reviews in Refs. 39 and 40). However, there is no any effective and universal technique for achieving parallel ordering of the molecular axes, i.e., orientation. There are just a few experiments on orientation of small molecules and best results are achieved

[a]Electronic mail: zhdanov@phys.msu.ru.
[b]Electronic mail: zadkov@phys.msu.ru.

so far in experiments with molecules cooled in a supersonic jet up to a few Kelvin at the joint action of laser and electrostatic fields.[41] Therefore, preparation of an ensemble of well-oriented molecules, which can be used further for the purpose of the AAS, for instance, is a separate very difficult experimental problem.

That is why most attention nowadays is paid to the development of the AAS scenarios, which are based exclusively on the use of electrodipole interaction with the laser field and do not require preliminary orientation of the molecules.[25–32] First step in this direction has been made in Ref. 25, where authors derived a general condition for the AAS scenarios of such kind. Soon after that, a few more specific laser-assisted AAS scenarios were proposed.[26–32] Their experimental realization seems, unfortunately, also difficult and none of them has been realized so far for the following reasons.

First of all, to be effective, all these scenarios require working temperatures of a few Kelvin[42] and most of them have been developed for the molecules with dynamical chirality.[27,29–32] Second, the AAS scenarios developed in Refs. 26–31 can be, in fact, experimentally applied only to the single spatially localized molecules. This is due to the fact that the direction of the AAS in these scenarios strongly depends on the position of the enantiomers, so that delocalization of the molecules in a spatial area of size comparable with the laser wavelengths leads to the complete loss of control of the AAS reaction. Finally, applications of the methods suggested in Refs. 25, 27, and 28 are limited only by molecules with achiral excited electronic states.

Taking into account all the above listed disadvantages of the available AAS scenarios, we suggest here a novel AAS scenario based on the electrodipole interaction of the incident laser field with chiral molecules. This scenario can be applied to nonoriented molecules having stable chiral configurations. It does not require rigid spatial localization of the molecules and their preliminary cooling. For developing this scenario, we first conducted a general analysis of the symmetry constrains on the parameters of the light-molecule interaction in the AAS scenarios, which employs only dipole active transitions. Section II summarizes the results of this symmetry study. A few symmetry conditions are derived that must be fulfilled in any laser-assisted AAS. These conditions help to develop novel or select existing AAS scenarios according to the molecule's specific features of the electrodipole transition structure as well as to make an optimal choice for polarizations and propagation directions for the laser field components. In Sec. III, we consider the basic component of the novel AAS scenario—exclusive excitation of preselected enantiomers in a racemic mixture based on the concept of the laser orientation-dependent selection of molecules proposed by us recently.[43] Also, qualitative description of the suggested AAS scenario is given. Detailed numerical analysis of this scenario on example of SiHNaClF chiral molecules, estimation of its efficiency, and possible experimental realization are discussed in Sec. IV. In Sec. V, we summarize key results and outline possible perspectives of the laser-assisted AAS scenarios.

II. GENERAL SYMMETRY ANALYSIS OF THE AAS SCENARIOS

In this section, we will analyze symmetry properties of the laser-assisted AAS of enantiomers from a racemic mixture of chiral molecules. For simplicity, let us consider a mixture of free gaseous chiral molecules. We assume that molecules in the mixture do not interact with each other and that they are initially in a thermodynamic equilibrium state characterized by the density matrix $\hat{\rho}_0$. Then, the photoinduced molecular dynamics is described by the transformation $U\hat{\rho}_0 U^{-1}$ with the evolution operator U of the form

$$U(\boldsymbol{\mathcal{E}}) = \mathcal{T}\exp\left[-\frac{i}{\hbar}\int_{-\infty}^{t}\hat{H}(\boldsymbol{\mathcal{E}})dt\right], \tag{1}$$

where $\mathcal{T}$ is the time ordering operator and the Hamiltonian $\hat{H}(\boldsymbol{\mathcal{E}})=\hat{H}_0+\hat{H}_I(\boldsymbol{\mathcal{E}})$ is the sum of the eigen-Hamiltonian of the molecule $\hat{H}_0$ and the Hamiltonian $\hat{H}_I(\boldsymbol{\mathcal{E}})$ describing electrodipole interaction with the incident laser field.

Our analysis will be based on revealing the general symmetry properties, which are intrinsic to the eigenstates of chiral molecules, and on investigation of the symmetry selection rules for electrodipole transitions in these molecules.

The AAS of enantiomers from a racemic mixture is an example of the process for which symmetry toward spatial inversion of molecular coordinates $\hat{E}^*$ is broken.[44] Operation $\hat{E}^*$ does not change the state of the racemic mixture of randomly oriented chiral molecules:

$$\hat{E}^*\hat{\rho}_0\hat{E}^{*-1} = \hat{\rho}_0. \tag{2}$$

At the same time, the density matrices $\hat{\rho}_L$ and $\hat{\rho}_D$, which describe similar ensembles of nonoriented L and D enantiomers, respectively, are not invariant with respect to $\hat{E}^*$ and connected to each other as $\hat{\rho}_{L(D)}=\hat{E}^*\hat{\rho}_{D(L)}\hat{E}^{*-1}$. This relation illustrates that under inversion the left-handed enantiomers $|L\rangle$ are transferred into the right-handed $|D\rangle$ and vice versa:

$$\hat{E}^*|L(D)\rangle = |D(L)\rangle. \tag{3}$$

As a quantitative measure of the AAS, we can use the so called degree of chirality, $\chi=(\mathcal{N}_L-\mathcal{N}_D)/(\mathcal{N}_L+\mathcal{N}_D)$, which characterizes the relative excess of the left-handed $(\mathcal{N}_L)$ to the right-handed $(\mathcal{N}_D)$ enantiomers in the mixture of chiral molecules. For a racemic mixture, it is equal to zero, whereas $\chi=+1$ $(\chi=-1)$ corresponds to the pure ensemble of $L(D)$ enantiomers.

An origin of the symmetry breaking of an initial state $\hat{\rho}_0$ can only be interaction with an external laser field. This is because the nonperturbed Hamiltonian $\hat{H}_0$ (up to negligibly small corrections due to the weak interactions) is invariant with respect to this transformation:

$$\hat{E}^{*-1}\hat{H}_0\hat{E}^* = \hat{H}_0. \tag{4}$$

Respectively, the eigenstates of a chiral molecule are always characterized with the definite parity: $\hat{E}^*|\Psi_k\rangle=|\Psi_k\rangle$, $\hat{E}^*|\Psi_{-k}\rangle=-|\Psi_{-k}\rangle$. Let us enumerate the eigenstates $\hat{H}_0$ with the integer index k $(-\infty<k<\infty, k\neq 0)$ in a way that positive and negative values of k correspond to the even and odd

functions, respectively, and that the values of all quantum numbers, except parities, are equal for the eigenstates $|\Psi_k\rangle$ and $|\Psi_{-k}\rangle$. From the comparison with Eq. (3) it is clear that not the pure eigenstates but their superposition corresponds to the enantiomers of a definite handedness:

$$|L_k\rangle = \frac{1}{\sqrt{2}}(|\Psi_k\rangle + |\Psi_{-k}\rangle), \quad |D_k\rangle = \frac{1}{\sqrt{2}}(|\Psi_k\rangle - |\Psi_{-k}\rangle) \quad (k>0). \tag{5}$$

Therefore, the states $|\Psi_k\rangle$ and $|\Psi_{-k}\rangle$ are called as chiral doublets.

Generally speaking, L and D enantiomers of free chiral molecules are not stable and transferred into each other at the time $\tau_{\text{tun}}=\pi\hbar/|E_{-k}-E_k|$. This time depends on the eigenenergy difference E_k and E_{-k} of the states $|\Psi_k\rangle$ and $|\Psi_{-k}\rangle$, respectively.[45]

In semiclassical electrodipole approximation, the interaction Hamiltonian $\hat{H}_I$ with the laser field is a bilinear combination of the vector characteristics of the molecules and the field: $\hat{H}_I(\boldsymbol{\mathcal{E}})=-\hat{\mathbf{d}}\boldsymbol{\mathcal{E}}$. Here $\hat{\mathbf{d}}$ is the dipole moment operator of the molecule and $\boldsymbol{\mathcal{E}}$ describes the laser field, which can, in general, have a multicomponent structure:

$$\boldsymbol{\mathcal{E}} = \sum_j \boldsymbol{\mathcal{E}}_j = 2\sum_j \boldsymbol{\varepsilon}_j A_j(t)\cos(\omega_j t+\varphi_j), \tag{6}$$

where $A_j(t)$ and ω_j are the amplitudes and frequencies of the respective components and $\boldsymbol{\varepsilon}_j$ are the unit vectors characterizing their polarization. Due to the relation $\hat{E}^{*-1}\hat{\mathbf{d}}\hat{E}^{*}=-\hat{\mathbf{d}}$, which is the consequence of the polar vector character of the dipole moment, and the bilinear structure of the interaction Hamiltonian, the result of application of the operator $\hat{E}^{*}$ to $\hat{H}_I$ is formally equal to the inversion of the configuration of the laser field:

$$\hat{E}^{*}\hat{H}_I(\boldsymbol{\mathcal{E}})\hat{E}^{*-1} = -\hat{H}_I(\boldsymbol{\mathcal{E}}) = \hat{H}_I(-\boldsymbol{\mathcal{E}}). \tag{7}$$

Using Eqs. (2)–(7) and repeating reasoning from Ref. 25, one can readily prove that the necessary condition for the laser-assisted AAS of enantiomers from a racemic mixture is the *noncoplanarity* of the incident laser field. In fact, the change of the degree of chirality due to the interaction with the incident laser field is given by the following formula:

$$\chi = \mathrm{Tr}[\hat{\chi}U(\boldsymbol{\mathcal{E}})\hat{\rho}_0 U^{-1}(\boldsymbol{\mathcal{E}})], \tag{8}$$

where operator of the degree of chirality $\hat{\chi}$ has the form

$$\hat{\chi} = \frac{1}{\mathrm{Tr}\,\rho}\sum_{k=1}^{\infty}|L_k\rangle\langle L_k| - |D_k\rangle\langle D_k| = \frac{1}{\mathrm{Tr}\,\rho}\sum_{k=-\infty}^{\infty}|\Psi_k\rangle\langle\Psi_{-k}|. \tag{9}$$

From Eq. (3), it follows that $\hat{E}^{*-1}\hat{\chi}\hat{E}^{*}=-\hat{\chi}$. Thus, taking into account Eqs. (2), (4), and (7) we have

$$\begin{aligned} -\chi &= \mathrm{Tr}[\hat{E}^{*-1}\hat{\chi}\hat{E}^{*}U(\boldsymbol{\mathcal{E}})\hat{\rho}_0 U^{-1}(\boldsymbol{\mathcal{E}})] \\ &= \mathrm{Tr}[\hat{\chi}(\hat{E}^{*}U(\boldsymbol{\mathcal{E}})\hat{E}^{*-1})\hat{\rho}_0(\hat{E}^{*}U(\boldsymbol{\mathcal{E}})\hat{E}^{*-1})^{-1}] \\ &= \mathrm{Tr}[\hat{\chi}U(-\boldsymbol{\mathcal{E}})\hat{\rho}_0 U^{-1}(-\boldsymbol{\mathcal{E}})]. \end{aligned} \tag{10}$$

Therefore, change of the signs of all the components of the laser field, i.e., inversion of the polarization configuration of the laser field, results in the change of the AAS direction. In the case of the coplanar polarization configuration of the incident laser field $\boldsymbol{\mathcal{E}}_{\text{copl}}$, when $\boldsymbol{\mathcal{E}}_{\text{copl}}(t)\perp\mathbf{n}_\perp$ ($\mathbf{n}_\perp$ is the spatially fixed vector), such inversion is equivalent to the rotation $R^{\pi}_{\mathbf{n}_\perp}$ of the laboratory reference frame at 180° around $\mathbf{n}_\perp$. In our case of randomly oriented chiral molecules, operators $\hat{H}_0$, $\hat{\chi}$, and the initial state $\hat{\rho}_0$ are invariant with respect to $R^{\pi}_{\mathbf{n}_\perp}$; thus, from Eq. (10) it follows that

$$\begin{aligned} -\chi &= \mathrm{Tr}[\hat{\chi}U(-\boldsymbol{\mathcal{E}}_{\text{copl}})R^{\pi}_{\mathbf{n}_\perp}\hat{\rho}_0(R^{\pi}_{\mathbf{n}_\perp})^{-1}U^{-1}(-\boldsymbol{\mathcal{E}}_{\text{copl}})] \\ &= \mathrm{Tr}[\hat{\chi}U(\boldsymbol{\mathcal{E}}_{\text{copl}})\hat{\rho}_0 U^{-1}(\boldsymbol{\mathcal{E}}_{\text{copl}})] = \chi, \end{aligned} \tag{11}$$

i.e., $-\chi=\chi=0$, which proves the validity of the above formulated condition.

Further analysis is targeted at the development of the more specific conditions for the laser-assisted AAS. It is based on a more thorough description of molecular symmetry and its role in affecting the photoexcitation process. Let us start with consideration of the general formula (8) for the degree of chirality and transferring it into the convenient for the further analysis form. For this, let us assume that an initial state of each chiral molecule in a racemic isotropic mixture is thermodynamically equilibrium, characterized by the temperature T, and described with the corresponding density matrix:

$$\hat{\rho}_0 = \sum_{k=-\infty}^{\infty} P_k|\Psi_k\rangle\langle\Psi_k|, \tag{12}$$

where $P_k=(\Sigma_{k=-\infty}^{\infty}e^{-E_k/(kT)})^{-1}e^{-E_k/(kT)}$.

The Hamiltonians $\hat{H}_0$ and $\hat{H}_I$ in the energy representation take then the form

$$\hat{H}_0 = \sum_{k=-\infty}^{\infty} E_k|\Psi_k\rangle\langle\Psi_k|, \quad \hat{H}_I = -\sum_{k,l=-\infty}^{\infty}\boldsymbol{\mathcal{E}}\mathbf{d}_{k,l}|\Psi_k\rangle\langle\Psi_l|, \tag{13}$$

where $\mathbf{d}_{k,l}=\langle\Psi_k|\hat{\mathbf{d}}|\Psi_l\rangle$. Let us then rewrite Eq. (8) in the interaction representation, which gives

$$\chi = \mathrm{Tr}[U_0^{-1}(t)\hat{\chi}U_0(t)\tilde{U}_I(\boldsymbol{\mathcal{E}})\hat{\rho}_0\tilde{U}_I^{-1}(t)]. \tag{14}$$

Here $U_0(t)=\exp[-(i/\hbar)\int_{-\infty}^{t}\hat{H}_0 dt]$, $\tilde{U}_I(t)=\mathcal{T}\exp[-(i/\hbar)\times\int_{-\infty}^{t}\tilde{\hat{H}}_I(\boldsymbol{\mathcal{E}},t)dt]$, and $\tilde{\hat{H}}_I(\boldsymbol{\mathcal{E}},t)$ has the form

$$\tilde{\hat{H}}_I(\boldsymbol{\mathcal{E}},t) = U_0^{-1}(t)\hat{H}_I(\boldsymbol{\mathcal{E}},t)U_0(t) = -\boldsymbol{\mathcal{E}}\sum_{k,l=-\infty}^{\infty}\mathbf{d}_{k,l}e^{i\omega_{k,l}t}|\Psi_k\rangle\times\langle\Psi_l|, \tag{15}$$

where $\omega_{k,l}=(1/\hbar)(E_k-E_l)$. From Eqs. (9) and (12)–(15), we finally receive

$$\chi = \sum_{N=1}^{\infty}\chi^{(N)}, \tag{16}$$

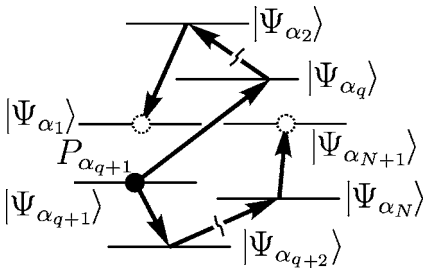

FIG. 1. The chain of transitions, which results under the laser excitation to the racemity breaking [see Eqs. (16)–(18)].

$$\chi^{(N)} = \sum_{\{\boldsymbol{\alpha}\}(N+1)} \left(e^{i\omega_{-\alpha_1,\alpha_1}t} \sum_{q=0}^{N} \frac{i^{-(N-2q)}}{\hbar^N} P_{\alpha_{q+1}} \times W(\boldsymbol{\alpha}(N+1),q,\boldsymbol{\mathcal{E}},t) \right), \tag{17}$$

$$W(\boldsymbol{\alpha}(N+1),q,\boldsymbol{\mathcal{E}},t) = \int_{-\infty}^{t} dt_1 \int_{-\infty}^{t_1} dt_2 \cdots \int_{-\infty}^{t_{q-1}} dt_q \times \int_{-\infty}^{t} dt_N \int_{-\infty}^{t_N} dt_{N-1} \cdots \int_{-\infty}^{t_{q+2}} dt_{q+1} \times \left[\delta_{\alpha_1,-\alpha_{N+1}} \prod_{p=1}^{N} \boldsymbol{\mathcal{E}}(t_p) \mathbf{d}_{\alpha_p,\alpha_{p+1}} e^{i\omega_{\alpha_p,\alpha_{p+1}}t_p} \right]. \tag{18}$$

In the last equation, $\delta_{\alpha,\beta}$ is the Kronecker delta function and $\Sigma_{\{\alpha\}(N+1)}$ designate summation across all possible sets of $N+1$ random integer (except zero) numbers α_p.

Physical essence of Eqs. (16)–(18) is that racemity breaking of the racemic mixture is caused by the formation of a coherent superposition of the chiral doublet states $|\Psi_{\alpha_1}\rangle$ and $|\Psi_{\alpha_{N+1}=-\alpha_1}\rangle$ due to the excitation of the chain of electrodipole transitions that coherently link these states via $N-1$ intermediate states $|\Psi_{\alpha_p}\rangle$, $2 \leqslant p \leqslant N$ (Fig. 1). It is obvious that existence of such chains, i.e., existence of nonzero products in squared brackets in Eq. (18), is the necessary condition for obtaining a nonzero value of χ after the laser action.

Let us clarify first which structure should the incident laser field have to satisfy this condition in a specific, but probably most interesting from practical point of view case of rigid stable chiral molecules. Hereafter, we will consider molecules as rigid ones if their deformations are negligible in a sense that one can entirely separate the rotational and vibronic variables in the Hamiltonian $\hat{H}_0$, at least during the laser action.

It is worth to note here that in this approximation, the AAS process cannot be described completely because in the AAS it is assumed that either one kind of enantiomers is converted into another one or enantiomers of a specific type are destroyed. It is obvious that such processes cannot be described, in general, with the help of the rigid molecule model. Nevertheless, this simple model in many cases describes well the energetic separations of enantiomers, the key stage of the AAS. During this stage, the enantiomers with preselected configuration are transferred into the well-separated group of excited states $|\Psi_{\tilde{k}}\rangle$, $\tilde{k} \in \tilde{\mathcal{K}}$ ($\tilde{\mathcal{K}}$ is the subset of these excited states indices), whereas the enantiomers of another configuration remain unexcited.[46] From mathematical point of view, this means that the degree of chirality after such separation remains always equal to zero. However, the partial degree of chirality χ' of excited molecules [described by Eq. (16), where one should restrict summation across the sets $\{\boldsymbol{\alpha}\}$ to the sets $\{\tilde{\boldsymbol{\alpha}}\}$ in which $\alpha_1 \in \tilde{\mathcal{K}}$] can be, in principle, different from zero. Energetic separation of the L and D enantiomers allows one to manipulate with them *independently* and, therefore, realize the AAS, for instance, with the help of enantioselective photodissociation or stereomutation scenarios in application to the excited enantiomers by using the standard techniques of coherent control.[29,30]

Eigen-Hamiltonian for the rigid molecule model, when we neglect spin-orbital interaction, can be written in the form

$$\hat{H}_0 = A\hat{J}_{x'}^2 + B\hat{J}_{y'}^2 + C\hat{J}_{z'}^2 + \hat{H}_0, \tag{19}$$

where A, B, and C are the rotational constants, $\hat{J}_{x'}$, $\hat{J}_{y'}$, and $\hat{J}_{z'}$ are the operators of the projections of the angular momentum on the respective axes of the molecule-fixed frame $\{x'y'z'\}$, and $\hat{H}_0$ is the vibronic Hamiltonian, which depends only on the intramolecular coordinates.

Symmetry properties of Hamiltonian (19) are well known:[47,48] it is invariant with respect to the spatial inversion transformation $\hat{E}^*$ of the coordinates of the atoms and electrons in the molecule, rotations $\hat{U}_{x'}^{\pi}$, $\hat{U}_{y'}^{\pi}$, and $\hat{U}_{z'}^{\pi}$ at 180° around each axis of the molecular frame, and to the mirror reflections $\hat{\sigma}_h^{x'}$, $\hat{\sigma}_h^{y'}$, and $\hat{\sigma}_h^{z'}$ of the coordinates of all the particles constituting the molecule in the planes perpendicular to the axes $\mathbf{x}'$, $\mathbf{y}'$, and $\mathbf{z}'$. All these symmetry transformations form the commutative group $\mathcal{G}$ (formally, isomorphic to the point group D_{2h}). Transformation properties of each eigenfunction of the Hamiltonian correspond to one of the eight one-dimensional irreducible representations of this group. To clarify the following consideration, we will explicitly indicate in the notations of the eigenfunctions their symmetry with respect to the transformations $\hat{\sigma}_h^{x'}$, $\hat{\sigma}_h^{y'}$, and $\hat{\sigma}_h^{z'}$ because it uniquely defines which of these representations they belong to. For this, let us define three indices $i_{x'}$, $i_{y'}$, and $i_{z'}$, which are equal to +1 when the state is symmetrical or to −1 when it is antisymmetrical with respect to these transformations. Then, the eigenfunctions $|\Psi_k\rangle$ of Hamiltonian (19) can be written in the form $|i_{x',k},i_{y',k},i_{z',k},\mathbf{n}_{|\mathbf{k}|}\rangle$, where $\mathbf{n}$ is the set of the rest of the quantum numbers describing the state. From Eqs. (5) and the fact that each of the operations $\hat{\sigma}_h^{x'}$, $\hat{\sigma}_h^{y'}$, and $\hat{\sigma}_h^{z'}$ transfers L enantiomer into the D enantiomer, one can easily see that the chiral doublets $|\Psi_k\rangle$ and $|\Psi_{-k}\rangle$ in the new notations are represented as $|i_{x',k},i_{y',k},i_{z',k},\mathbf{n}_{|k|}\rangle$ and $|-i_{x',k},-i_{y',k},-i_{z',k},\mathbf{n}_{|\mathbf{k}|}\rangle$, i.e.,

$$i_{\xi,-k} = -i_{\xi,k} \quad (\xi = x',y',z'), \quad i_{x',k}i_{y',k}i_{z',k} = \mathrm{sign}(k). \tag{20}$$

Let us then investigate the character of perturbation of the free molecule's dynamics due to the interaction of the

molecule with a laser field. For this, we will expand the dipole moment operator to its projections on the axes of the molecule-fixed frame:

$$\hat{\mathbf{d}}_0 = \hat{\boldsymbol{\epsilon}}_{x'}\hat{d}_{x'} + \hat{\boldsymbol{\epsilon}}_{y'}\hat{d}_{y'} + \hat{\boldsymbol{\epsilon}}_{z'}\hat{d}_{z'},$$

where the unit vector operators along with the corresponding axes $\hat{\boldsymbol{\epsilon}}_{\xi'}$ $(\xi'=x',y',z')$ depend only on the angle variables and operators $\hat{d}_{\xi'}$ depend only on the intramolecular variables. Then, one can readily show that the operators $\hat{\boldsymbol{\epsilon}}_{x'}\hat{d}_{x'}$, $\hat{\boldsymbol{\epsilon}}_{y'}\hat{d}_{y'}$, and $\hat{\boldsymbol{\epsilon}}_{z'}\hat{d}_{z'}$ are transferred in accordance with the irreducible representations B_{1u}, B_{2u}, and B_{3u} of the group $\mathcal{G}$ (representation notations are given by analogy with those of the D_{2h} group), i.e., similar to the states $|-1,1,1,\mathbf{n}_{k'}\rangle$, $|1,-1,1,\mathbf{n}_{k''}\rangle$, and $|1,1,-1,\mathbf{n}_{k'''}\rangle$, respectively. Keeping this in mind, after definition of the symmetry of the corresponding direct products of the representations and application of the selection rules, one can readily find general form of the nonzero matrix elements of the dipole moment operator:

$$\langle i_{x'},i_{y'},i_{z'},\mathbf{n}_k|\hat{\boldsymbol{\epsilon}}_{x'}\hat{d}_{x'}|-i_{x'},i_{y'},i_{z'},\mathbf{n}_l\rangle,$$

$$\langle i_{x'},i_{y'},i_{z'},\mathbf{n}_k|\hat{\boldsymbol{\epsilon}}_{y'}\hat{d}_{y'}|i_{x'},-i_{y'},i_{z'},\mathbf{n}_l\rangle,$$

$$\langle i_{x'},i_{y'},i_{z'},\mathbf{n}_k|\hat{\boldsymbol{\epsilon}}_{z'}\hat{d}_{z'}|i_{x'},i_{y'},-i_{z'},\mathbf{n}_l\rangle. \tag{21}$$

Therefore, the dipole transition is allowed between basis states with coinciding arbitrary two out of three quantum numbers $i_{x'}$, $i_{y'}$, and $i_{z'}$, and different third number $i_{\xi'}$. With this, the corresponding direction of the transition dipole moment is collinear with the main axis $\boldsymbol{\xi}'$ of the tensor of inertia of the molecule.

Now, we are ready to elucidate the condition of the energetic separation of the enantiomers in an isotropic racemic mixture. Suppose that a set of indices $\{\boldsymbol{\alpha}\}(N+1)$ is chosen to meet the requirement of the nonzero product in squared brackets in Eq. (18). Let us denote in the corresponding chain of transitions as $N_{x'}$, $N_{y'}$, and $N_{z'}$ the number of transitions, dipole moments of which are collinear to the axes $\mathbf{x}'$, $\mathbf{y}'$, and $\mathbf{z}'$, respectively. Then, from Eq. (21) it follows that

$$i_{\xi,\alpha_{N+1}} = i_{\xi,\alpha_1}(-1)^{N_\xi} \quad (\xi = x',y',z'),$$

$$\mathrm{sign}(\alpha_{N+1}) = (-1)^{N_{x'}+N_{y'}+N_{z'}}\,\mathrm{sign}(\alpha_1).$$

Keeping in mind that $\alpha_{N+1}=-\alpha_1$ and using properties (20), we obtain that not only N but also each of N_ξ are to be different from zero and be odd. Thus, we can formulate the following three conditions of (partial) racemity breaking.

(i) The AAS (energetical separation) in the isotropic racemic mixture of chiral molecules can be achieved only as a result of $(2n+1)$-photon processes (n is a natural number) that link coherently the states of the chiral doublets by the chain of dipole transitions.

(ii) Configurational structure of the transition dipole moments of each of these multiphoton transitions must be noncoplanar.

(iii) Each of the three components $\hat{\boldsymbol{\epsilon}}_{x'}\hat{d}_{x'}$, $\hat{\boldsymbol{\epsilon}}_{y'}\hat{d}_{y'}$, and $\hat{\boldsymbol{\epsilon}}_{z'}\hat{d}_{z'}$ of the dipole moment must be responsible for the odd number of transitions.

Note that while deriving conditions (i)–(iii), we made no assumption about the value of the energetic separation between the states in the chiral doublets. Therefore, these conditions are also valid for the nonrigid molecules with dynamical chirality, if approximation (19) is fulfilled. Also note that in the latter case, the energetic separation of enantiomers, as a rule, leads directly to the racemity breaking[31,32] because of the rapidly-oscillating factor $e^{i\omega_{-\alpha_1,\alpha_1}t}$ in Eq. (17).

Let us show that condition (i) is valid not only for the rigid top molecules, but is a universal condition of the racemity breaking in isotropic media. For this, it is necessary to prove only that in Eq. (16) all $\chi^{(N)}$, for which $N=1$ and $N=2n$, where n is an arbitrary natural number, are equal to zero. Note that due to the isotropic character of an initial state, the degree of induced chirality χ is invariant with respect to the arbitrary rotations of the polarization configuration of the incident laser field $\boldsymbol{\mathcal{E}}$ independent of its form. In addition, since the values of $\chi^{(N)}$ with various N, being functionals of the various field powers, are linearly undependable, then each $\chi^{(N)}$ must also be invariant with respect to such rotations. At $N=1$, we have

$$\chi^{(1)} = \sum_{\alpha=-\infty}^{\infty}\left(e^{i\omega_{-\alpha,\alpha}t}\frac{-i}{\hbar}(P_\alpha - P_{-\alpha})\int_{-\infty}^{t} dt_1[(\boldsymbol{\mathcal{E}}_x(t_1) + \boldsymbol{\mathcal{E}}_y(t_1) + \boldsymbol{\mathcal{E}}_z(t_1))\mathbf{d}_{\alpha,-\alpha}e^{i\omega_{\alpha,-\alpha}t_1}]\right). \tag{22}$$

Here, the laser field $\boldsymbol{\mathcal{E}}$ is presented as a sum of its projections on the laboratory frame axes $\{xyz\}$. Invariance with respect to the rotations of the polarization configuration of the incident laser field at 180° along axes x, y, and z means that

$$\chi^{(1)} = \sum_{\alpha=-\infty}^{\infty}\left(e^{i\omega_{-\alpha,\alpha}t}\frac{-i}{\hbar}(P_\alpha - P_{-\alpha})\int_{-\infty}^{t} dt_1[(\boldsymbol{\mathcal{E}}_x(t_1) - \boldsymbol{\mathcal{E}}_y(t_1) - \boldsymbol{\mathcal{E}}_z(t_1))\mathbf{d}_{\alpha,-\alpha}e^{i\omega_{\alpha,-\alpha}t_1}]\right),$$

$$\chi^{(1)} = \sum_{\alpha=-\infty}^{\infty}\left(e^{i\omega_{-\alpha,\alpha}t}\frac{-i}{\hbar}(P_\alpha - P_{-\alpha})\int_{-\infty}^{t} dt_1[(-\boldsymbol{\mathcal{E}}_x(t_1) + \boldsymbol{\mathcal{E}}_y(t_1) - \boldsymbol{\mathcal{E}}_z(t_1))\mathbf{d}_{\alpha,-\alpha}e^{i\omega_{\alpha,-\alpha}t_1}]\right),$$

$$\chi^{(1)} = \sum_{\alpha=-\infty}^{\infty}\left(e^{i\omega_{-\alpha,\alpha}t}\frac{-i}{\hbar}(P_\alpha - P_{-\alpha})\int_{-\infty}^{t} dt_1[(-\boldsymbol{\mathcal{E}}_x(t_1) - \boldsymbol{\mathcal{E}}_y(t_1) + \boldsymbol{\mathcal{E}}_z(t_1))\mathbf{d}_{\alpha,-\alpha}e^{i\omega_{\alpha,-\alpha}t_1}]\right).$$

Summing up these three equalities and comparing with Eq. (22), we get $-\chi^{(1)}=\chi^{(1)}$, i.e., $\chi^{(1)}=0$, which proves our statement for $N=1$. The fact that all $\chi^{(N)}$ are equal to zero at $N=2n$ follows from condition on the parity conservation in the act of emission/absorption of a photon. In fact, as the photon parity is negative, then in each such act of emission/absorption the parity of the molecule's state must be changed. Therefore, none of the states $|\Psi_k\rangle$ and $|\Psi_{-k}\rangle$, which always have the opposite parities, cannot be linked with a chain of the one-photon transitions, if the number of these transitions is even. However, such chains are used for summing up in Eq. (16) for even N, from which the proof of our statement follows.

Conditions (i)–(iii) are useful for the development of the AAS scenarios because they help to reveal either one or another AAS scenario works or not just from general information about its structure. For example, the analysis of the AAS scenario suggested in Ref. 25 immediately shows that it does not work properly for isotropic media.

Let us clarify then which structure should the incident laser field [Eq. (6)] have. We will limit ourselves to the case when the dominating contribution to the excitation of the dipole transition between any two states $|\Psi_k\rangle$ and $|\Psi_l\rangle$ is due to the only one field component with the frequency $\omega_{j(k,l)}$. Therefore, the analysis of the photoinduced dynamics can be performed in the rotating wave approximation (RWA). Then, Eq. (18) takes the form

$$W(\boldsymbol{\alpha}(N+1),q,\boldsymbol{\mathcal{E}},t)=\int_{-\infty}^{t}dt_1\int_{-\infty}^{t_1}dt_2\cdots\int_{-\infty}^{t_{q-1}}dt_q\int_{-\infty}^{t}dt_N\int_{-\infty}^{t_N}dt_{N-1}\cdots\int_{-\infty}^{t_{q+2}}dt_{q+1}$$
$$\times\left[\delta_{\alpha_1,-\alpha_{N+1}}\prod_{p=1}^{N}\boldsymbol{\varepsilon}_{j(\alpha_p,\alpha_{p+1})}\mathbf{d}_{\alpha_p,\alpha_{p+1}}A_{j(\alpha_p,\alpha_{p+1})}(t)\times e^{i\,\mathrm{sign}(\omega_{\alpha_p,\alpha_{p+1}})(\Delta(j(\alpha_p,\alpha_{p+1}),\alpha_p,\alpha_{p+1})t_p+\varphi_{j(\alpha_p,\alpha_{p+1})})}\right], \tag{23}$$

where $\Delta(j,\alpha_p,\alpha_{p+1})=\omega_j-|\omega_{\alpha_p,\alpha_{p+1}}|$ is the frequency detuning from the resonance. One can then readily formulate the following condition for the AAS.

(iv) Let us assume that $\mathcal{J}'$ is a set of indices of the k laser field components with directions $\boldsymbol{\varepsilon}_{j'}$ of the polarization vectors orthogonal to the plane $\mathcal{S}$ and n is the number of transitions in the chain of transitions induced by these k components. Then, n has to be odd if the directions of polarization vectors of remaining components lie in $\mathcal{S}$.

To prove this condition, consider a mirror image of the polarization configuration of the laser field components with respect to the plane $\mathcal{S}$. This operation is equivalent (with accuracy up to the rotation transformation) to inversion of the polarization configuration. Therefore, on the one hand, due to Eq. (10) the result of such transformation should be equivalent to the change in the induced degree of chirality $\chi\rightarrow-\chi$, but, on the other hand, such transformation changes the signs of all the components $\boldsymbol{\mathcal{E}}_{j'}$, $j'\in\mathcal{J}'$. Thus, from Eq. (23) we have $W(\boldsymbol{\alpha},q,\boldsymbol{\mathcal{E}},t)\rightarrow(-1)^nW(\boldsymbol{\alpha},q,\boldsymbol{\mathcal{E}},t)$ and, respectively, $\chi\rightarrow(-1)^n\chi$. The required proof readily follows from comparison of these two consequences.

We can derive also a simple rule for selecting the polarization configuration of the multicomponent incident laser field for the AAS scenarios, when the quantum character and dynamics of the rotations can be neglected. In this case, the AAS process is well described in the model of the frozen molecules in which the photoinduced dynamics of a single molecule depends parametrically on the set of fixed angular variables $\boldsymbol{\vartheta}$ characterizing its orientation. The action on the ensemble of molecules, as a whole, is determined then via a plain statistical averaging over $\boldsymbol{\vartheta}$. Conditions at which such simplified description is valid are fulfilled in an important from the practical point of view case when the AAS is arranged at the normal conditions with the help of strong femtosecond pulses. In this case, the typical rotational energy significantly exceeds the value of rotational quanta and the duration of the laser pulses τ_{las} is significantly shorter than a typical period of molecular rotation.

Let us redefine as $\hat{H}_0$ the respective reduced eigen Hamiltonian of the vibronic dynamics of the molecule. We also assume that $|\psi_k(\boldsymbol{\vartheta})\rangle$ are its eigenvectors, which correspond to the states with vibronic energies E_k, and then $\hat{H}_I=-\boldsymbol{\mathcal{E}}\hat{\mathbf{d}}(\boldsymbol{\vartheta})$ is the reduced interaction Hamiltonian, where everywhere the dependence on $\boldsymbol{\vartheta}$ is a parametric one. For the following, we rewrite the matrix elements $\mathbf{d}_{k,l}(\boldsymbol{\vartheta})=\langle\psi_k(\boldsymbol{\vartheta})|\hat{\mathbf{d}}(\boldsymbol{\vartheta})|\psi_l(\boldsymbol{\vartheta})\rangle$ of the redefined reduced dipole moment operator $\hat{\mathbf{d}}(\boldsymbol{\vartheta})$ in the form $\mathbf{d}_{k,l}(\boldsymbol{\vartheta})=\boldsymbol{\epsilon}_{k,l}(\boldsymbol{\vartheta})\mathrm{d}_{k,l}$, where $\mathrm{d}_{k,l}=|\mathbf{d}_{k,l}|$. Calculations similar to Eqs. (12)–(15) then lead to the expression for the degree of chirality similar to Eqs. (16) and (17), but in which $W(\boldsymbol{\alpha}(N+1),q,\boldsymbol{\mathcal{E}},t)$ takes the form

$$W(\boldsymbol{\alpha}(N+1),q,\boldsymbol{\mathcal{E}},t)=\int_{-\infty}^{t}dt_1\int_{-\infty}^{t_1}dt_2\cdots\int_{-\infty}^{t_{q-1}}dt_q\int_{-\infty}^{t}dt_N\int_{-\infty}^{t_N}dt_{N-1}\cdots\int_{-\infty}^{t_{q+2}}dt_{q+1}$$
$$\times\left[\delta_{\alpha_1,-\alpha_{N+1}}\left\langle\prod_{p=1}^{N}\boldsymbol{\varepsilon}_{j(\alpha_p,\alpha_{p+1})}\boldsymbol{\epsilon}_{\alpha_p,\alpha_{p+1}}(\boldsymbol{\vartheta})\right\rangle_{\boldsymbol{\vartheta}}\prod_{p=1}^{N}\mathrm{d}_{\alpha_p,\alpha_{p+1}}A_{j(\alpha_p,\alpha_{p+1})}(t)\right.$$
$$\left.\times e^{i\,\mathrm{sign}(\omega_{\alpha_p,\alpha_{p+1}})(\Delta(j(\alpha_p,\alpha_{p+1}),\alpha_p,\alpha_{p+1})t_p+\varphi_{j(\alpha_p,\alpha_{p+1})})}\right]. \tag{24}$$

Angular brackets $\langle\cdots\rangle_{\boldsymbol{\vartheta}}$ denote here the statistical averaging across all possible orientations of the molecules. From Eq. (24), one can readily derive the following necessary condition of the AAS.

(v) The directions $\boldsymbol{\epsilon}_{k,l}$ of the transition dipole moments and polarizations $\boldsymbol{\varepsilon}_{j(\alpha_k,\alpha_l)}$ of the respective components of the incident laser field in the chain of transitions coherently linking the states $|\psi_{\alpha_1}(\boldsymbol{\vartheta})\rangle$ and $|\psi_{\alpha_{N+1}=-\alpha_1}(\boldsymbol{\vartheta})\rangle$ must satisfy the inequality

$$\left\langle\prod_{p=1}^{N}\boldsymbol{\varepsilon}_{j(\alpha_p,\alpha_{p+1})}\boldsymbol{\epsilon}_{\alpha_p,\alpha_{p+1}}(\boldsymbol{\vartheta})\right\rangle_{\boldsymbol{\vartheta}}\neq 0. \tag{25}$$

In order to verify condition (25), one needs to perform an analysis of the matrix elements of the dipole transitions between symmetrized states, which is not always suitable because interpretation of these symmetrized states $|\psi_k(\boldsymbol{\vartheta})\rangle$ is not always transparent. Thus, it is more useful, in general, to analyze the transition matrix elements $\mathbf{d}^{l}_{k,l}(\boldsymbol{\vartheta})=\langle l_{|k|}(\boldsymbol{\vartheta})|\hat{\mathbf{d}}(\boldsymbol{\vartheta})|l_{|l|}(\boldsymbol{\vartheta})\rangle$ and $\mathbf{d}^{d}_{k,l}(\boldsymbol{\vartheta})=\langle d_{|k|}(\boldsymbol{\vartheta})|\hat{\mathbf{d}}(\boldsymbol{\vartheta})|d_{|l|}(\boldsymbol{\vartheta})\rangle$ between the localized states $|l_k(\boldsymbol{\vartheta})\rangle$ and $|d_k(\boldsymbol{\vartheta})\rangle$, corresponding to the L and D enantiomers, which are defined similar to Eq. (5). In particular, while considering the energetic separation of the enantiomers with stable chiral configurations, all matrix elements of the form $\langle l_k(\boldsymbol{\vartheta})|\hat{\mathbf{d}}(\boldsymbol{\vartheta})|d_l(\boldsymbol{\vartheta})\rangle=0$ can be usually assumed to be equal to zero, because the wavepackets corresponding to the respective localized states almost do not overlap. In this case, using Eqs. (3) and (5) and taking into account that $\mathbf{d}_{k,l}(\boldsymbol{\vartheta})=0$ for $k\times l>0$, one can easily show that $\mathbf{d}_{k,l}(\boldsymbol{\vartheta})=\mathbf{d}^{l}_{k,l}(\boldsymbol{\vartheta})=-\mathbf{d}^{d}_{k,l}(\boldsymbol{\vartheta})$. Respectively, condition (25) can be written in the more convenient form

$$\left\langle\prod_{p=1}^{N}\boldsymbol{\varepsilon}_{j(\alpha_p,\alpha_{p+1})}\boldsymbol{\epsilon}^{l}_{\alpha_p,\alpha_{p+1}}(\boldsymbol{\vartheta})\right\rangle_{\boldsymbol{\vartheta}}-\left\langle\prod_{p=1}^{N}\boldsymbol{\varepsilon}_{j(\alpha_p,\alpha_{p+1})}\boldsymbol{\epsilon}^{d}_{\alpha_p,\alpha_{p+1}}(\boldsymbol{\vartheta})\right\rangle_{\boldsymbol{\vartheta}}\neq 0. \tag{26}$$

In addition to the frequency and polarization properties of the incident laser field, the phase relationships between its components are also decisive for the AAS process. In fact, from Eq. (18) it follows that the dependence of $W(\boldsymbol{\alpha}(N+1),q,\boldsymbol{\mathcal{E}},t)$ on the phases φ_j has the form

$$W(\boldsymbol{\alpha}(N+1),q,\boldsymbol{\mathcal{E}},t)\propto\prod_{p=1}^{N}e^{i\,\mathrm{sign}(\omega_{\alpha_p,\alpha_{p+1}})\varphi_{j(\alpha_p,\alpha_{p+1})}}.$$

It is obvious that if the phases do not match, then the averaged values $W(\boldsymbol{\alpha}(N+1),q,\boldsymbol{\mathcal{E}},t)$ are equal to zero. The values of the phases φ_j depend on the position of the molecule: $\varphi_j=\varphi_j^0-\mathbf{k}_j\mathbf{r}$, where $\mathbf{r}$ is the radius vector of the center of mass of the molecule and $\mathbf{k}_j$ is the wavevector of the jth field component. Therefore, for the AAS in an ensemble of chiral molecules for which the delocalization area is comparable to (at the order of value or exceeds) the characteristic wavelength of the incident laser field, the following phase matching condition must be fulfilled:

$$\sum_{p=1}^{N}\mathrm{sign}(\omega_{\alpha_p,\alpha_{p+1}})\mathbf{k}_{j(\alpha_p,\alpha_{p+1})}=0. \tag{27}$$

Note that, on the other hand, for the stable chiral molecules the energetic separation in the chiral doublets is negligible. Therefore, the resonance condition for the chain of transitions [Eq. (18)] connecting the states of the chiral doublets has the form

$$\sum_{p=1}^{N}\mathrm{sign}(\omega_{\alpha_p,\alpha_{p+1}})\omega_{j(\alpha_p,\alpha_{p+1})}=0. \tag{28}$$

Let us consider the case when we can neglect the dispersion of the phase velocities, so that $\omega_j=|\mathbf{k}_j|c$. From conditions (27) and (28), it seems at hand that for solving the phase matching problem, one simply needs that the wavevectors of all three components of the incident laser field coincide, i.e., $\mathbf{k}_j\|\boldsymbol{\kappa}$ $(j=1,2,\ldots)$. Under such choice, however, the polarizations of all the field components would lie in the plane perpendicular to $\boldsymbol{\kappa}$, i.e., the noncoplanarity requirement of the polarization configuration of the incident laser field cannot be fulfilled. Therefore, the structure of the incident laser field must fulfill the following condition.

(vi) The incident laser field must consist of a set of two or more subsets $(u,v,\ldots)$ of the components with different frequencies. The wavevectors of all the components in any u subset should be collinear to the direction $\boldsymbol{\kappa}_u$ $(|\boldsymbol{\kappa}_u|=1)$, and $\boldsymbol{\kappa}_u\neq\boldsymbol{\kappa}_w(u\neq w)$. Also, for the components of each subset, the following phase matching condition must be fulfilled:

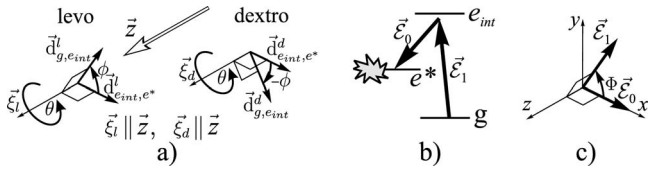

FIG. 2. AAS of enantiomers from a racemic mixture of chiral molecules. (a) Spatial configuration of the matrix elements of the dipole transitions between working levels in the oriented enantiomers. (b) Laser excitation scheme. (c) Polarization configuration of the laser field components.

$$\sum_{p=1}^{N} \delta(\mathbf{k}_{j(\alpha_p,\alpha_{p+1})}/|\mathbf{k}_{j(\alpha_p,\alpha_{p+1})}|,\boldsymbol{\kappa}_u)\mathrm{sign}(\omega_{\alpha_p,\alpha_{p+1}})\omega_{j(\alpha_p,\alpha_{p+1})} = 0. \quad (29)$$

III. AAS SCENARIO BASED ON THE LASER ORIENTATION-DEPENDENT SELECTION OF CHIRAL MOLECULES

In this section, we will use the above derived general conditions for the AAS for elaboration of a rather universal scenario of the AAS from racemic mixtures, which is based on the electrodipole interaction of molecules with an intense pulsed laser radiation. We will limit our consideration to the case of molecules having stable chiral configurations and consider the roughest strategy of laser distillation of a racemic mixture when an excess of the enantiomers of a given handedness is achieved by the selective photodestruction of the enantiomers of the opposite handedness. We also assume that the photodestruction of the molecules is due to their photoinduced transfer to the antibonded excited vibronic states.

The suggested AAS scenario is based on combination of the methods of coherent control in oriented chiral molecules[8–21,25–32] and the concept of the laser orientation-dependent selection of molecules developed by us earlier.[43]

To clarify the idea of the method, let us consider the dynamics of the AAS on example of an abstract stable chiral molecule. For a qualitative analysis of the AAS mechanism, it is not necessary to specify details of the vibrational dynamics of the molecule. Also we suppose that its rotational dynamics can be treated in the model of the frozen molecules considered in Sec. II.

We will show first how the AAS can be realized for the oriented molecules. Let us assume that the molecules have three electronic levels g, e_{int}, and e^* that correspond to the ground and two excited states of the molecule for which transitions $g \leftrightarrow e_{\mathrm{int}}$ and $e_{\mathrm{int}} \leftrightarrow e^*$ are allowed and that the molecules in the excited state e^* dissociate rapidly. Denote the molecule-fixed axis in the L enantiomers, which is orthogonal to the directions of the matrix elements $\mathbf{d}^l_{g,e_{\mathrm{int}}}$ and $\mathbf{d}^l_{e_{\mathrm{int}},e^*}$ of the dipole moment, as $\boldsymbol{\xi}_l$. It is obvious that configuration formed by these three vectors and configuration of the corresponding vectors $\boldsymbol{\xi}_d$, $\mathbf{d}^d_{g,e_{\mathrm{int}}}$, and $\mathbf{d}^d_{e_{\mathrm{int}},e^*}$ in D enantiomers should be mirror images of each other. Let us also assume that we somehow oriented the molecules in a racemic mixture in a way that the axes $\boldsymbol{\xi}_l$ and $\boldsymbol{\xi}_d$ coincide with the spatially fixed axis $\mathbf{z}$ (see Fig. 2) (molecules can still freely rotate around the $\mathbf{z}$ axis).

Let us show that if the angle between directions of the matrix elements of the dipole moments of the transitions $g \leftrightarrow e_{\mathrm{int}}$ and $e_{\mathrm{int}} \leftrightarrow e^*$ is different from zero and π, then the action of the two-component laser field $\boldsymbol{\mathcal{E}}_0+\boldsymbol{\mathcal{E}}_1$ with the corresponding frequencies ω_0 and ω_1, tuned into the resonance with the two-photon transition $g \rightarrow e^*$ via the intermediate level e_{int}, can excite the L and D enentiomers with different efficacy. To prove this, let us assume that the field components are linearly polarized in the plane perpendicular to $\mathbf{z}$, so that the angle between directions of their polarizations is equal to Φ [Fig. 2(c)]. Assuming probabilities P^l_{diss} and P^d_{diss} of photodissociation of the L and D enantiomenrs proportional to the probability of the two-photon transition to the state e^*, we have

$$P^l_{\mathrm{diss}} \propto \langle|(\boldsymbol{\mathcal{E}}_1\mathbf{d}^l_{g,e_{\mathrm{int}}}(\theta))(\boldsymbol{\mathcal{E}}_0\mathbf{d}^l_{e_{\mathrm{int}},e^*}(\theta))|^2\rangle_\theta,$$

$$P^d_{\mathrm{diss}} \propto \langle|(\boldsymbol{\mathcal{E}}_1\mathbf{d}^d_{g,e_{\mathrm{int}}}(\theta))(\boldsymbol{\mathcal{E}}_0\mathbf{d}^d_{e_{\mathrm{int}},e^*}(\theta))|^2\rangle_\theta, \quad (30)$$

where averaging is taken across all possible values of the angle θ describing rotations of the molecules around axis $\mathbf{z}$. After averaging over θ, Eqs. (30) take the form

$$P^{l,d}_{\mathrm{diss}} \propto \cos(2(\phi \mp \Phi)) + 2. \quad (31)$$

From this equation, it follows that the photoinduced decay rates of the L and D enantiomers are, generally speaking, different. One can easily show that the major difference is realized at the values $\phi, \Phi = \pm\pi/4, \pm 3\pi/4$, when the ratio of the decay rates reaches 3. As a result, an excess of the enantiomers with the slower photodestruction rates will be formed.

Therefore, for building up the AAS scenario, which will work at room temperature, we should first eliminate in the described scheme the requirement to the axes $\boldsymbol{\xi}_l$ and $\boldsymbol{\xi}_d$ of the molecules to be parallel to the $\mathbf{z}$ axis, which is rather difficult to realize in experiment nowadays (see the Introduction). In order to solve this problem, we will properly modify the scheme of the laser orientation-dependent selection of molecules.[43] This scheme allows us to make selective manipulations (even at the room temperatures) with molecules of the required orientation in an ensemble of randomly oriented molecules. It is based on the transfer of the molecules having the required spatial orientation in the separate subensemble. Molecules in this subensemble are distinguishable from others by their specific internal state. This state should be chosen in a way that allows independent manipulations with the molecules in the subensemble. In general case, such subensemble must be dynamically refreshed as the molecules change their orientation during free thermal motion.

Key disadvantages of the selection scheme proposed in Ref. 43 are the need in electrostatic field with the amplitude close to the molecular ionization threshold and the specific requirements to the molecular permanent dipole moment behavior under the laser excitation. The latter significantly narrows the types of molecules for which this scheme could be applied.

In this work, a novel variant of the laser scheme of orientation-dependent selection of molecules is proposed,

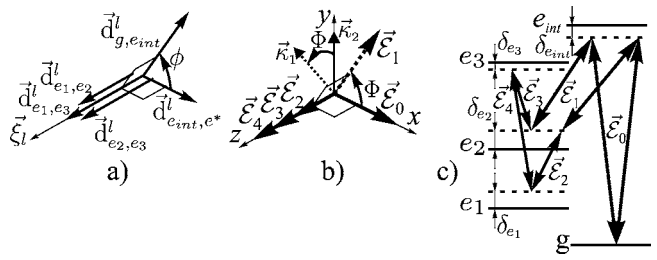

FIG. 3. The AAS scenario based on the laser orientation-dependent selection of molecules. (a) Spatial configuration of the matrix elements of the dipole moments for the used in the AAS chain of transitions. (b) Polarization configuration of the incident laser field. (c) Scheme of the laser-induced transitions.

which does not require electrostatic field. In this variant, selection of molecules is arranged by the final state of the photoinduced process, which we have to make orientation dependent. In other words, we produce such photoinduced changes in the structure of the final state of this process that its realization becomes possible only for the specifically oriented molecules. We will show that this modified selection scheme allows us to extend the ideas of the above considered scheme of the AAS in oriented molecules onto the case of randomly oriented chiral molecules. For this, we need to organize the special orientation-dependent modification of the parameters of the state e^*, so that the transition $e_{\text{int}} \leftrightarrow e^*$ would be allowed only for the molecules with the directions of axis $\boldsymbol{\xi}_l$ or $\boldsymbol{\xi}_d$ close to the direction of the $\mathbf{z}$ axis; otherwise, this transition is disabled.

Such dependence in our scheme results from the phase matched action of three additional intense laser fields $\boldsymbol{\mathcal{E}}_2$, $\boldsymbol{\mathcal{E}}_3$, and $\boldsymbol{\mathcal{E}}_4$. Their frequencies should satisfy the relation $\omega_4 = \omega_2 + \omega_3$ and be chosen in a way that some three electronic states e_1, e_2, and e_3 of the molecule become coherently linked with each other via the electrodipole transitions [Fig. 3(c)]. Let us also require that the parameters of the state e_2 and of the laser fields $\boldsymbol{\mathcal{E}}_1$ and $\boldsymbol{\mathcal{E}}_0$ satisfy all the conditions for the selective two-photon excitation of oriented enantiomers to the electronic state e_2, except for the large frequency detuning δ_2 from the two-photon resonance for the transition $g \leftrightarrow e_2$. The latter prevents the molecule's excitation into the state e_2 in the absence of the additional field components $\boldsymbol{\mathcal{E}}_2$, $\boldsymbol{\mathcal{E}}_3$, and $\boldsymbol{\mathcal{E}}_4$. However, the presence of these additional components leads to modification of the eigen-electronic-states e_1, e_2, and e_3 of the molecule and, as a result, the fields $\boldsymbol{\mathcal{E}}_0$ and $\boldsymbol{\mathcal{E}}_1$ interact now with the dressed states, which structure and effective energies are determined by the amplitudes and polarizations of the fields $\boldsymbol{\mathcal{E}}_2$, $\boldsymbol{\mathcal{E}}_3$, and $\boldsymbol{\mathcal{E}}_4$, as well as by the configuration of the matrix elements of the transitions between levels e_1, e_2, and e_3, and, therefore, depend on the molecule's orientation. This dependence is in the core of our scheme.

In order to select the molecules according to their orientation, one should choose levels e_1 and e_3 in a way that the matrix elements of the dipole transitions $\mathbf{d}^{l(d)}_{e_1,e_2}$, $\mathbf{d}^{l(d)}_{e_2,e_3}$, and $\mathbf{d}^{l(d)}_{e_1,e_3}$ are parallel to $\boldsymbol{\xi}_l$ ($\boldsymbol{\xi}_d$). The direction of the polarization of the additional field components should be collinear to the axis $\mathbf{z}$ [Figs. 3(a) and 3(b)].

Dynamics of the laser action on the molecules is characterized by the Hamiltonian $\hat{H} = \hat{H}_{\text{dressed}} - \hat{\mathbf{d}}(\boldsymbol{\mathcal{E}}_0 + \boldsymbol{\mathcal{E}}_1)$, where $\hat{H}_{\text{dressed}} = \hat{H}_0 - \hat{\mathbf{d}}(\boldsymbol{\mathcal{E}}_2 + \boldsymbol{\mathcal{E}}_3 + \boldsymbol{\mathcal{E}}_4)$ describes free molecule's dynamics taking into account additional laser field components. In the RWA and with the help of representation (6), $\hat{H}_{\text{dressed}}$ reads as

$$\hat{H}^l_{\text{dressed,RWA}}(\varphi) = \hbar\Bigg(0|l_g\rangle\langle l_g| + \delta_{e_{\text{int}}}|l_{e_{\text{int}}}\rangle\langle l_{e_{\text{int}}}| + \sum_{k=1}^{3}\delta_{e_k}|l_{e_k}\rangle \times\langle l_{e_k}|\Bigg) - [d_{e_1,e_2}A_2\cos(\varphi)e^{i\varphi_2}|l_{e_1}\rangle\langle l_{e_2}| + d_{e_2,e_3}A_3\cos(\varphi)e^{i\varphi_3}|l_{e_2}\rangle\langle l_{e_3}| + d_{e_1,e_3}A_4\cos(\varphi)e^{i\varphi_4}|l_{e_1}\rangle\langle l_{e_3}| + \text{H.c.}] \tag{32}$$

for the L enantiomers and is given by almost identical expression for the D enantiomers (except swapping the indices $l \leftrightarrow d$). Here, $d_{k,l} = d^l_{k,l} = d^d_{k,l}$, values of δ_j are determined by the frequency detunings of the laser field components from the resonance, and angle $\varphi = \widehat{\boldsymbol{\xi}_{l(d)}, \mathbf{z}}$ characterizes the orientation of the molecule with respect to the polarization direction of the additional field components. The possibility of orientation-dependent selection is based on the parametric dependence of eigenenergies and eigenvectors of the dressed states, corresponding to Hamiltonian (32), on φ. Let us denote one of these dressed states as e^*, i.e., identify it with the state e^* in the above considered AAS scenario. Its structure is described with the linear combination of the form

$$|l_{e^*}\rangle = C_1(\varphi)|l_{e_1}\rangle + C_2(\varphi)|l_{e_2}\rangle + C_3(\varphi)|l_{e_3}\rangle, \tag{33}$$

where coefficients C_k depend parametrically on the angle φ as well as on the phases and amplitudes of the additional field components.

In the following, we will assume that the parameters of the field are set to guarantee that for all the values of φ eigenvector (33) corresponds to the eigenvalue $\hbar\delta_{e^*}$ of Hamiltonian (32) (which is the effective energy of the state e^*), which is significantly different from the effective energies of the two other eigenstates e' and e'' so that one can neglect the transitions $g \to e_{\text{int}} \to e'$ and $g \to e_{\text{int}} \to e''$ due to the large frequency detunings from the resonance. In this case, the problem of the laser orientation-dependent selection of molecules is reduced to the problem of finding such parameters of laser pulses at which the two-photon transition $g \to e_{\text{int}} \to e^*$ at large values of φ becomes ineffective either due to the small value of the matrix element $|\mathbf{d}_{e_{\text{int}},e^*}|$ or due to the large frequency detuning δ_{e^*} from the resonance for the two-photon transition $g \to e_{\text{int}} \to e^*$. As the modulus of the matrix element $\mathbf{d}_{e_{\text{int}},e^*}$ can be written as the product $|\mathbf{d}_{e_{\text{int}},e^*}| = |C_2||\mathbf{d}_{e_{\text{int}},e_2}|$, the condition of its small value can be rewritten as $C_2 \to 0$.

Let us now find the parameters of the laser action at which the coefficient C_2 goes to zero for the molecules, which orientations are orthogonal ($\varphi = \pi/2$) and opposite ($\varphi = \pi$) to the required orientation. For $\varphi = \pi/2$, all nondiagonal elements of Hamiltonian (32) are equal to zero and,

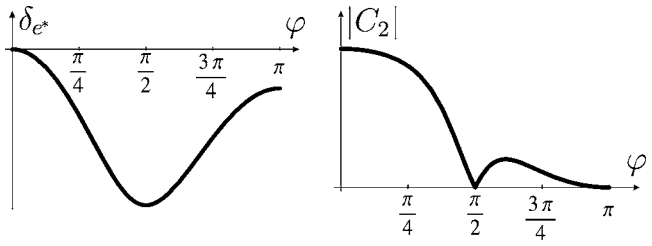

FIG. 4. Typical dependence of the detuning δ_{e^*} and the coefficient $|C_2|$ on the orientation angle φ at the parameters of the incident laser fields fitting the conditions for the laser orientation-dependent selection of molecules.

therefore, the corresponding dressed states coincide with the eigenfunctions of $\hat{H}_0$. Therefore, for zeroing C_2 it is necessary that the dressed state $|l_{e^*}\rangle$ at $\varphi=\pi/2$ is transferred either into the state $|l_{e_1}\rangle$ or to $|l_{e_3}\rangle$. For $\varphi=\pi$, substituting $C_2=0$ in the equation $\hat{H}^l_{\text{dressed,RWA}}|l_{e^*}\rangle=\hbar\delta_{e^*}|l_{e^*}\rangle$, we receive the following relationship between the amplitude components $\boldsymbol{\mathcal{E}}_2$, $\boldsymbol{\mathcal{E}}_3$, and $\boldsymbol{\mathcal{E}}_4$ and the optimal frequency detuning of the component $\boldsymbol{\mathcal{E}}_4$ from the resonance, as well as the relationship between the phases of the additional field components:

$$A_4=\frac{\hbar(\delta_{e_1}-\delta_{e_3})d_{e_1,e_2}d_{e_2,e_3}}{d_{e_1,e_3}\left(\frac{A_3}{A_2}d^2_{e_1,e_2}-\frac{A_2}{A_3}d^2_{e_2,e_3}\right)},\quad \varphi_4=\varphi_2+\varphi_3. \tag{34}$$

At last, the optimal value of the frequency detuning δ_{e_2} is determined from the condition $\delta_{e^*}(\varphi=0)=0$.

Typical dependences of $|C_2|$ and δ_{e^*} on φ for the laser interaction parameters determined from the above relationships are shown in Fig. 4. One can see that the detuning δ_{e^*} is small in the region of angles $0<\varphi<\pi/4$ and the amplitude of the coefficient C_2 reaches its maximum, i.e., the most favorable conditions for the excitation of the transition $g\rightarrow e^*$ are achieved. With increasing the value of φ, the detuning δ_{e^*} also promptly increases, whereas the amplitude of $|C_2|$ promptly decreases; thus, in the region of angles $\pi/4<\varphi<\pi/2$ this transition becomes blocked. Further increasing the angle φ up to π is accompanied by a significant reduction of the detuning δ_{e^*}; however, the value of $|C_2|$ at the whole interval becomes small, so that the probability of the transition $g\rightarrow e^*$ still remains small. Therefore, only those molecules actively interact with the fields $\boldsymbol{\mathcal{E}}_0$ and $\boldsymbol{\mathcal{E}}_1$ whose orientation is characterized by the small values of φ, which means that we realized the orientation-dependent selection of molecules.

For further analysis of the AAS, we will use the symmetry conditions derived in Sec. II. Let us first check if condition (v), i.e., inequality (26), is fulfilled or not. One can show with the help of Figs. 3(a) and 3(b) and simple calculations that the shortest (and, respectively, making the most essential contribution to the AAS process) chain of transitions coherently linking the chiral doublets for which the above inequality can be fulfilled has the structure indicated by the bold arrows in Fig. 3. This chain obviously fulfills condition (i). Inequality (26) in this case has the form $4/105\sin(2\Phi)\sin(2\phi)\neq 0$. Therefore, for the AAS is it necessary that Φ, $\phi\neq n\pi/2$ (n is an integer number). One can easily note that at the values $\Phi=n\pi/2$, condition (iv) fails. Moreover, at odd n one more condition for the noncoplanarity of the polarization configuration of the laser fields fails and the values $\phi=n\pi$ do not fulfill condition (iii). Amplitude values in the left side of condition (26) are achieved for ψ, $\Psi=\pm\pi/4$, $\pm 3\pi/4$, which strictly correspond to the optimal parameters of the AAS obtained from Eq. (31).

For completing the analysis of the AAS scheme, it is necessary to determine the directions of the laser field component propagation. It seems to be most optimal to use multicomponent laser field impact, which is composed of two laser pulses: first pulse, less intensive and longer than the second one, contains component $\boldsymbol{\mathcal{E}}_1$, and has a longitudinal profile close to the rectangular one. Its propagation direction $\boldsymbol{\kappa}_1$ lies in the plane xy and sets an angle Φ with axis $\mathbf{y}$ [parameters of this pulse are shown by dashed arrows in Fig. 3(b)]. Direction $\boldsymbol{\kappa}_2$ of propagation of the second laser pulse is parallel to the axis $\mathbf{y}$. This pulse is shorter than the first one, more intensive, and consists of four components $\boldsymbol{\mathcal{E}}_0$, $\boldsymbol{\mathcal{E}}_2$, $\boldsymbol{\mathcal{E}}_3$, and $\boldsymbol{\mathcal{E}}_4$ [shown by solid arrows in Fig. 3(b)]. Time profiles of each of these four components can be Gaussian:

$$A_j=a_1\exp(-2(t-t_0)^2/\tau_j^2), \tag{35}$$

where the relationship $\tau_0<\tau_2,\tau_3,\tau_4$ is important.

For this configuration of the laser fields, both the number of the laser pulses and the angle between directions of their propagation achieve their minimum. Therefore, the overlapping region between laser pulses, where the AAS takes place, is maximal for such configuration. Space dimensions of the area in which the AAS is initiated are determined also by the duration and space profiles of the laser pulses. Increasing the duration of the pulses, however, leads simultaneously with enlarging the AAS area to enlarging the areas through which the laser pulses propagate without overlapping. The latter leads to the increase of various parasitic nonresonant processes caused by each of the pulses separately and significantly reduces the quality of the AAS. Thus, the component durations τ_1 of about a few picoseconds and τ_2, τ_3, and τ_4 on the order of 10^2 fs seem to be optimal for the majority of cases. Also, the frequency detuning $\delta_{e_{\text{int}}}$ of the first pulse from the resonance must be chosen essentially large in order to suppress the unwanted excitation of the molecules into the state e_{int}. In this case, propagation of the first pulse itself will not significantly affect the vibronic dynamics of molecules. When the first and second pulses are overlapped, action of the field components $\boldsymbol{\mathcal{E}}_2$, $\boldsymbol{\mathcal{E}}_3$, and $\boldsymbol{\mathcal{E}}_4$ results in formation of the dressed states e^*, e', and e''. Then, the component $\boldsymbol{\mathcal{E}}_0$, having shorter duration, overlaps with the pulse $\boldsymbol{\mathcal{E}}_1$ and produces the selective two-photon excitation $g\rightarrow e^*$. By and large, the whole duration of the population transfer is determined by the duration of the second pulse, and, therefore, is on the order of $\sim 10^2$ fs. As a rule, this time is significantly shorter than the characteristic period of molecular rotations, which confirms the validity of describing the AAS process with the help of the frozen molecule model.

In order to fulfill the second relationship in Eq. (34) a phase matching of the components $\boldsymbol{\mathcal{E}}_2$, $\boldsymbol{\mathcal{E}}_3$, and $\boldsymbol{\mathcal{E}}_4$ is required. One can easily check that in the case when dispersion is absent the fulfillment of the second relationship in Eq. (34) at the considered configuration of the laser pulses automati-

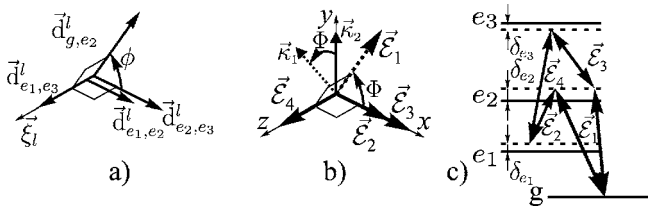

FIG. 5. Another variant of the AAS scenario. (a) Spatial configuration of the matrix elements of the dipole moment for the used in the AAS scenario transitions. (b) Polarization configuration of the laser field components. (c) Scheme of the laser-induced transitions.

cally means fulfillment of all the phase matching conditions (29). Thus, the phase matching of the components $\boldsymbol{\mathcal{E}}_0$ and $\boldsymbol{\mathcal{E}}_1$ between each other and with the components $\boldsymbol{\mathcal{E}}_2$, $\boldsymbol{\mathcal{E}}_3$, and $\boldsymbol{\mathcal{E}}_4$ is not required.

This circumstance is extremely important because it gives a principal possibility of realization of the AAS in a volume with dimensions essentially larger than the wavelength of the laser radiation.

The above considered variant of the AAS scheme cannot be always applied to a specific molecule. For instance, in SiHNaClF molecule (considered in the next section), it is impossible to choose the levels e_1, e_2, and e_3 in a way that the matrix elements of the dipole transitions between them are parallel. In this case, one can use an alternative variant of the AAS scheme shown in Fig. 5.

Key difference of this scheme from the one considered above is that the matrix elements of the dipole moments $\mathbf{d}^{l(d)}_{e_1,e_2}$ and $\mathbf{d}^{l(d)}_{e_2,e_3}$ now are orthogonal to $\boldsymbol{\xi}_{l(d)}$. This leads to the respective change in the choice of the polarizations of the components $\boldsymbol{\mathcal{E}}_2$ and $\boldsymbol{\mathcal{E}}_3$. Also, this results in the qualitative difference in the AAS scheme, i.e., the condition of the laser orientation-dependent selection of molecules is now not only that the vector $\boldsymbol{\xi}_l$ or $\boldsymbol{\xi}_d$ is parallel to axis **z** but also that the directions of the matrix elements $\mathbf{d}^{l(d)}_{e_1,e_2}$ and $\mathbf{d}^{l(d)}_{e_2,e_3}$ are collinear to the polarization direction of the components $\boldsymbol{\mathcal{E}}_2$ and $\boldsymbol{\mathcal{E}}_3$, i.e., to axis **x**. This condition is, obviously, more restrictive, and therefore, we can simplify the AAS scheme using for excitation of the molecules into the state e^* the one-photon transition (instead of biharmonic pumping by $\boldsymbol{\mathcal{E}}_1$ and $\boldsymbol{\mathcal{E}}_0$) induced by the single component $\boldsymbol{\mathcal{E}}_1$. Polarization direction of $\boldsymbol{\mathcal{E}}_1$ now should be orthogonal to $\boldsymbol{\xi}_{l(d)}$ and set the angle Φ with the polarization directions of the components $\boldsymbol{\mathcal{E}}_2$ and $\boldsymbol{\mathcal{E}}_3$. Inequality (26) for the major chain of transitions coherently linking the chiral doublets [Fig. 5(c)] has, with the accuracy up to the coefficient, the previous form $2/35\sin(2\Phi)\sin(2\phi)\neq 0$. Thus, the optimal values of angles Φ and ϕ remain the same. Also the same are the conditions for choosing the amplitudes and frequencies of the components $\boldsymbol{\mathcal{E}}_2$, $\boldsymbol{\mathcal{E}}_3$, and $\boldsymbol{\mathcal{E}}_4$, specifically, formula (34) remains valid. As a result, besides the absence of the component $\boldsymbol{\mathcal{E}}_0$ and change of the polarization of the components $\boldsymbol{\mathcal{E}}_2$ and $\boldsymbol{\mathcal{E}}_3$, the structure and optimal directions of propagation of the respective laser pulses do not undergo any significant change: optimal laser impact, as before, consists of two laser pulses: the first pulse includes the component $\boldsymbol{\mathcal{E}}_1$ and propagates in the plane xy at the angle 45° toward the **y** axis, whereas the second pulse setting of the components $\boldsymbol{\mathcal{E}}_2$, $\boldsymbol{\mathcal{E}}_3$, and $\boldsymbol{\mathcal{E}}_4$ propagates along the **y** axis [Fig. 5(b)].

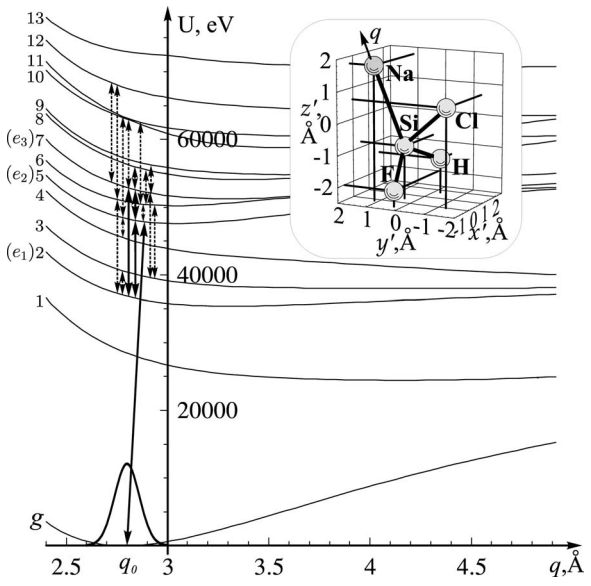

FIG. 6. Dependence of the electronic energy of SiHNaClF molecule vs the Na–Si bond length. Continuous arrows show the major working transitions in the suggested AAS scheme, whereas the dashed arrows indicate additional transitions for which the laser frequencies lie near the resonance frequencies. Also, the vibrational wavepacket is shown schematically for the ground state of the molecule. The inset shows the equilibrium configuration of one of the enantiomers of the molecule in the coordinate frame $\{x'y'z'\}$ of the major inertia tensor axes.

In the next section, we will use the last scenario for the analysis of the efficacy of the AAS from a racemic mixture on example of a specific molecule.

IV. NUMERICAL MODELING OF THE AAS SCENARIO FOR AN INITIALLY RACEMIC MIXTURE ON EXAMPLE OF SiHNaClF MOLECULES

Molecule SiHNaClF (Fig. 6) has been chosen by us for further theoretical analysis for several reasons.[49]

First, among molecules having stable chirality, this molecule is one of the simplest, and therefore, this circumstance significantly simplifies quantum-mechanical computations of the relevant molecular parameters (equilibrium configuration, electronic terms, transition dipole moments, etc.).

Second, satisfactory description of the vibrational dynamics of the nuclear subsystem for the early times after the excitation can be obtained with the help of a simple one-dimensional model in which the bond length Na–Si serves as a generalized vibrational coordinate q. Such a model allows us to significantly reduce the computational time during the computer modeling.

Third, we can describe the dynamics of the AAS process using the frozen molecule model. In fact, the characteristic rotational frequency of the SiHNaClF molecule at the temperature $T=300$ K is about 3.3×10^{11} Hz and thus the typical

rotational time scale (~3 ps) is one order of magnitude longer than the characteristic time of the photoinduced AAS process (~100 fs), so the conditions for applicability of the frozen molecule model are satisfied.

Finally, an important point is that the lowest excited electronic states of the molecule are well separated (energy gaps are larger than >0.35 eV) and weekly bound. The equilibrium value of the coordinate q for these states significantly differs from the equilibrium value q_0 in the ground electronic state g. Therefore, transfer of the molecule into these excited electronic states with the help of short laser pulses is accompanied by its strong vibrational excitation energy which is comparable with the energies of the respective vibrational potential barriers. As a result, one could expect that such excitation will lead with high probability to the dissociation of the molecules, which allows us to use the low-lying electronic states as the states e_1, e_2, and e_3 in the scheme of laser orientation-dependent selection. Significant energy gaps between these states also significantly suppress the role of the parasitic, nonresonant transitions at the early time after the excitation.

We model the laser-induced vibronic dynamics of the molecules using the Born-Oppenheimer approximation in the frame of the one-dimensional model of the vibrational dynamics with single generalized coordinate q. Information on the equilibrium molecular configuration and on the coordinate dependences of the electronic energy and matrix elements of the dipole moment of the electronic transitions have been obtained with the help of quantum-mechanical calculations software package GAUSSIAN 03.[50,51] Calculated equilibrium molecular configuration and vibrational potential energy surfaces are shown in Fig. 6.

From the analysis of calculated data, we found that the parameters of the second, fifth, and seventh excited electronic states correspond by and large to the requirements to the states e_1, e_2, and e_3, respectively, in the AAS scheme shown in Fig. 5. Using the results of Sec. III, we have found the corresponding optimal parameters of the laser field. The detailed inspection of these parameters shows, however, that in the case of the equilibrium molecular configuration the frequencies of the components $\boldsymbol{\mathcal{E}}_2$, $\boldsymbol{\mathcal{E}}_3$, and $\boldsymbol{\mathcal{E}}_4$ become close to the resonance frequencies for a number of additional transitions between the excited electronic states: $2\leftrightarrow3$, $2\leftrightarrow5$, $3\leftrightarrow5$, $3\leftrightarrow6$, $4\leftrightarrow5$, $5\leftrightarrow6$, $5\leftrightarrow10$, $5\leftrightarrow11$, $6\leftrightarrow8$, $6\leftrightarrow10$, $6\leftrightarrow11$, $6\leftrightarrow12$, $7\leftrightarrow8$, $7\leftrightarrow9$, $7\leftrightarrow10$, $7\leftrightarrow11$, $7\leftrightarrow12$ (Fig. 6). Therefore, in the calculations, we used an extended basis, which includes besides the ground electronic state g also 11 low-lying excited electronic states (from 2nd to 12th). Dynamics of the nuclear subsystem in each electronic state was described using grid representation of the wavefunctions (grid step is about 10^{-2} Å). Temporal dynamics of the molecule was calculated using standard symmetric split-operator method.[52,53]

Significant difference in the equilibrium bond lengths Na–Si for the ground and for most of excited electronic states (Fig. 6) greatly affects the dynamics of the photoinduced excitation of the molecules. The ground state vibrational wavefunction is localized in the vicinity of $q=q_0$ with the characteristic size of ~0.13 Å. After the laser excitation, excited vibrational wavepacket quickly leaves the vicinity of q_0 at the characteristic time τ_{out}, which is about few dozens of femtoseconds for the working terms 2 and 7, for instance. Excited vibrational states of the ground electronic state g are almost not involved into the photoinduced dynamics of the molecule at $q \gg q_0$ because the corresponding wavepackets do not overlap and the resonance conditions are significantly violated. Therefore, the total number of excited molecules is determined mostly by the dynamics of the vibronic interaction in the vicinity of $q=q_0$. Respectively, the characteristic time τ_{out} serves here as an effective longitudinal relaxation time.

These features imply essential limitations on the parameters of the laser action: since the required condition for the orientation-dependent laser selection of molecules is the creation and maintaining the coherent superposition of the electronic states 2, 5, and 7, then controlling the detunings $(1/\hbar)\delta_{e_1}$, $(1/\hbar)\delta_{e_2}$, $(1/\hbar)\delta_{e_3}$, $(1/\hbar)\delta_{e^*}$ and the effective Rabi frequencies of the transitions between these states should be greater or equal to the value of $1/\tau_{\text{out}}$. In order to fulfill this condition, the intensity of each selective components of the laser field $\boldsymbol{\mathcal{E}}_2$, $\boldsymbol{\mathcal{E}}_3$, and $\boldsymbol{\mathcal{E}}_4$ should be greater than 10^{11} W/cm^2. On the other hand, it is well known that the intensity of 10^{12} W/cm^2 is the typical threshold value above which the parasitic ionization processes start to play significant role in the photoinduced dynamics. Respectively, the optimal values of the intensities of the components $\boldsymbol{\mathcal{E}}_1$, $\boldsymbol{\mathcal{E}}_2$, $\boldsymbol{\mathcal{E}}_3$ of the dressing field should lie in the interval $10^{11}-10^{12}$ W/cm^2, and the controlling detunings should be on the order of 10^3 cm^{-1}. An important requirement while choosing the frequencies of the laser components is also the absence of significant resonances with the electronic states (in the vicinity of $q\sim q_0$), which are not involved in the AAS scheme.

Taking all these limitations into account, the following frequencies have been chosen for further calculations: $\omega_1=1.391\times10^{15}$ Hz ($\lambda_1=215.6$ nm), $\omega_2=3.297\times10^{14}$ Hz ($\lambda_2=909.3$ nm), $\omega_3=1.282\times10^{14}$ Hz ($\lambda_3=2339.1$ nm), and $\omega_4=4.579\times10^{14}$ Hz ($\lambda_4=654.8$ nm). The temporal profile of the components $\boldsymbol{\mathcal{E}}_2$, $\boldsymbol{\mathcal{E}}_3$, and $\boldsymbol{\mathcal{E}}_4$ is assumed Gaussian [see Eq. (35)] with $\tau_2=\tau_3=\tau_4=141$ fs. As the peak intensities for the field components we took $I_1^0=2.62\times10^9$ W/cm^2, $I_2^0=I_3^0=1.17\times10^{11}$ W/cm^2, and $I_4^0=4.28\times10^{11}$ W/cm^2, which in accordance with Sec. III should be optimal for the chosen frequencies. However, it is clear that these values are lower than the real optimal values because they were estimated without taking into account spreading of the vibronic wavepackets and parasitic influence of the transitions to electronic states, which were not included into the respective analysis in Sec. III. Therefore, we analyzed various sets of the maximal intensities of the form $I_j=\mu I_j^0$ ($j=2,3,4$) and the optimal value of the coefficient μ was elaborated based on the computer modeling results.

The time profile of the component $\boldsymbol{\mathcal{E}}_1$ is assumed rectangular with the front and rear sloping:

$$A_1 = a_1 \times \begin{cases} \frac{1}{2}[1-\cos(\pi(t+\tau_1/2)/\delta\tau_1)], & -\tau_1/2 < t < -\tau_1/2+\delta\tau_1 \\ 1, & -\tau_1/2+\delta\tau_1 < t < \tau_1/2-\delta\tau_1 \\ \frac{1}{2}[1+\cos(\pi(t-\tau_1/2)/\delta\tau_1)], & \tau_1/2-\delta\tau_1 < t < \tau_1/2. \end{cases} \quad (36)$$

The duration of the sloping and peak intensity of this pulse have been chosen from conditions $\delta\tau_1 \gg 1/\delta_{e_2}$ and $d_{g,e_2}A_1 \ll \hbar\delta_{e_2}$. At these conditions, the action of the only component $\boldsymbol{\mathcal{E}}_1$ leads to insignificant nonresonant adiabatic population of the fifth excited electronic state, which in our AAS scheme is the state e_2 (Fig. 6). For computer modeling, we used the following values: $\delta\tau_1 = 120$ fs, $I_1 < 6\times10^9$ W/cm^2, and $\tau_1 = 1-5$ ps. Calculations for the action of only $\boldsymbol{\mathcal{E}}_1$ component confirm that at the chosen parameters, a small population of the fifth excited electronic state during the excitation practically does not depend on the pulse duration. After ending the laser action, the majority of excited molecules adiabatically return into the ground state so that the remaining ratio of excited molecules does not exceed 10^{-5}.

Dynamical picture of the photoexcitation qualitatively changes when both first and second laser pulses act simultaneously (Fig. 5), because the frequency of the component $\boldsymbol{\mathcal{E}}_1$ becomes resonant (for the molecules with a specific orientation) for the excitation of molecules into the dressed state e^*. As a result, during a short time a fast nonadiabatic transfer and population redistribution across various excited electronic states take place. Vibronic wavepackets corresponding to the majority of these states rapidly move into the region of $q \gg q_0$. In this region, new resonances arise due to the essential change of the electronic terms energy, which lead to the complex processes of population redistribution and to the involvement into dynamics of the high-lying electronic states that are not included into the AAS calculation scheme. In addition, at the time scale necessary for population transfer into the region of the large values of q, the one-dimensional approximation for vibrational dynamics of the molecule is not valid. With this, the calculation scheme we use cannot guarantee the correct description of the population dynamics of the excited states and the dynamics of the dissociation of photoexcited molecules. Therefore, our estimations for the AAS efficiency have been made in a rough assumption that the dissociation probability of molecules is proportional to the total population of all excited electronic states after laser impact. With this assumption, one can introduce $\mathcal{R} = P_l/P_d$ as the AAS efficiency measure, where P_l and P_d are the excitation probabilities for the left- and right-handed enantiomers averaged over all possible molecular orientations.

Figure 7 illustrates the calculated dependences of P_l, P_d, and $\mathcal{R}$ on the intensities of the components of the second laser pulse for two different intensities of the first pulse. Comparing these dependences, one can conclude that despite the monotonic growth of the excitation probability for both enantiomers, increasing intensity of the first laser pulse practically does not change the ratio of these probabilities. Respectively, the AAS efficiency remains almost the same for the whole range of intensities of the second pulse. In Fig. 7(b), one can also see that the optimal intensities of the components of the second laser pulse, corresponding to the peak value $\mathcal{R} \sim 1.38$, approximately two times differ from those predicted from the analysis of the results of Sec. III.

Analysis of the laser action dynamics shows that this essential difference is mainly due to the parasitic quasiresonant interaction between the working electronic terms and the excited electronic states 3, 6, 10, and 11 (Fig. 6). Additional calculations show that if we can somehow exclude the possibility of photoinduced excitation of these states, then the optimal value of μ would be reduced to 1.3 and, therefore, becomes close to 1. At the same time, the value of $\mathcal{R}$ would be raised up to 1.85, so that the additional resonances greatly reduce the efficacy of the AAS.

In a real experiment, the total efficiency of the AAS will significantly depend on the transverse intensity distribution in each of the laser pulses as well as on the spatial distribution of the molecules in the active volume. In order to clarify these dependences, let us consider a case of the Gaussian cross section of both laser pulses with the half-width (at the level e^{-1}) for the first pulse equal to r_1 and for each component of the second pulse equal to r_2. Let us also suppose that the molecular concentration is maximal at the crossing point of the laser beam axes and falls from that point as $\exp(-r^2/r_0^2)$, where r is the distance to the crossing point.

As a characteristic of the total AAS efficiency in all the active volume, we will use $\mathcal{R}_s = \langle P_l\rangle_s/\langle P_d\rangle_s$, where the angular brackets $\langle\cdots\rangle_s$ indicate averaging over the whole macroscopic ensemble of molecules. The dependence of $\mathcal{R}_s$ on the ratio between the size of the molecules localization area and the characteristic transverse size of the laser beams is demonstrated in Fig. 8. In Fig. 8(a), one can see that the AAS runs most efficiently at r_1, $r_2 \gg r_0$. This is because in this case, all the molecules are localized in the vicinity of the axes of the laser pulses and are subject to approximately the same laser intensity action. Therefore, the conditions for the optimal action can be fulfilled for the whole ensemble of

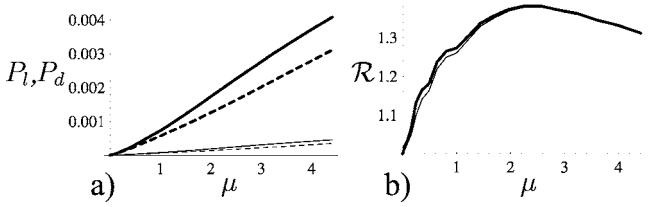

FIG. 7. (a) Probabilities P_d (continuous lines) and P_l (dashed lines) vs the coefficient μ, which characterizes the intensity of the second pulse (see the text). (b) Efficacy $\mathcal{R}$ of the AAS scheme vs the coefficient μ. The results in both left and right panels are given for two different peak intensities of the first laser pulse: 6.6×10^8 W/cm^2 (thin lines) and 5.9×10^9 W/cm^2 (bold lines).

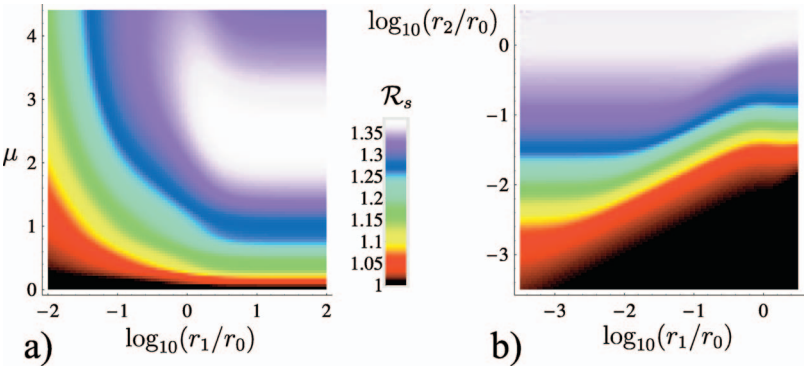

FIG. 8. (Color) (a) Efficiency $\mathcal{R}_s$ of the AAS scheme in the macroscopic volume vs the ratio between the characteristic sizes r_1 and r_0 and vs the intensity of the second laser pulse (parameter μ) in an assumption that the cross sections of the first and second pulses are equal: $r_1=r_2$. (b) Efficacy $\mathcal{R}_s$ vs the ratio between the radii of each of the laser pulses and the size of the localization area of the molecules at $\mu=3.24$.

molecules. With reducing r_1 and r_2, such conditions cannot be fulfilled simultaneously due to the increased number of molecules, which feel more weak laser action from the peripheral parts of the laser pulses. As a result, optimal intensity components for components of the second pulse grow up with simultaneous decreasing of r_1 and r_2.

The dependence of the AAS efficiency on the ratio between r_1 and r_2 is shown in Fig. 8(b). The character of this dependence at $r_2 \gtrsim r_0$ is determined by the fact that the local efficiency $\mathcal{R}$, as we have seen above, does not depend on intensity of the first pulse. Therefore, in the case when the intensity of the second pulse is approximately equal for all molecules in the ensemble, which is valid at $r_2 \gtrsim r_0$, the AAS efficiency does not depend on r_1. At $r_2 \ll r_0$ the situation is changed qualitatively. Such behavior is because the propagation of the first pulse itself is accompanied by excitation of a small fraction of molecules into the excited electronic state 5. Related to this process, parasitic photodissociation has quite low probability; however, it becomes a dominant factor when a part V_1 of the active volume, which is spanned by the first laser pulse, significantly exceeds the volume V_D of the region in which both pulses are overlapped and where the AAS takes place, i.e., in the case when $r_2 \ll r_0$. The ratio V_D/V_1 grows with increasing the ratio r_2/r_1, so that for $r_2 \ll r_0$ the AAS efficiency increases with decreasing r_1. We should also note that even at $r_1, r_2 \ll r_0$, the AAS efficiency can reach rather high values. For example, at $r_1=10^{-3}r_0$, $r_2=10^{-2}r_0$, and $\mu=4.41$, the efficiency $\mathcal{R}_s$ equals 1.2. This means that in an experiment with the laser pulses the cross sections of which are about 100 μm and 1 mm, respectively, the active volume with chiral molecules would have a characteristic size of up to 10 cm.

As one can see in Fig. 7, the effect of a single action of a pair of laser pulses even of high intensity is rather small. Therefore, let us now consider a question which value of the degree of chirality χ in the mixture of chiral molecules can be achieved as a result of numerously repeated action of the pair of laser pulses in the AAS scheme. As soon as the AAS process is accompanied by the destruction of a fraction of molecules, then improving the quality of the AAS should lead to the decrease in the useful output. Let us introduce $\eta=N_f/N_0$, which characterizes the ratio of the number of molecules N_f after ending the AAS toward their initial number N_0. A simple analysis shows that the values η, χ, and $\mathcal{R}_s$ are related to each other through the following relationship:

$$\eta=[(1-\chi)(1+\chi)^{-\mathcal{R}_s}]^{1/(\mathcal{R}_s-1)}. \tag{37}$$

Plotted with the help of this relationship, dependences of the induced degree of chirality χ versus η for several values of $\mathcal{R}_s$ are shown in Fig. 9. Assuming that for the case of SiHNaClF molecules the value $\mathcal{R}_s$ is about 1.3, one can easily see that for achieving a noticeable nonracemity in the mixture of chiral molecules, which is characterized by $\chi \sim 0.2$, we need to destroy about $\frac{4}{5}$ of the initial number of the molecules. At the same time, for achieving the same values of χ at $\mathcal{R}_s \sim 2$ (we have seen that such values of $\mathcal{R}_s$ could be achieved at the suppression of the interaction with additional electronic states), we should destroy less than half of the molecules. Therefore, one could expect that the more detailed calculations of the interaction parameters, which include an additional optimization of the methods for choosing the frequencies of the laser pulse components and the intensities of the components of the second pulse, will give us a possibility to significantly increase the AAS efficacy.

V. CONCLUSIONS

In conclusion, analysis of symmetry properties of the laser electrodipole interaction with chiral molecules resulted in a number of obligatory conditions on the parameters of such interaction for feasibility of the AAS from a racemic mixture of randomly oriented chiral molecules. For any chiral molecule, it is proved that the AAS is feasible only with the use of the multicomponent laser field with noncoplanar polarization configuration, which must coherently link the states of the chiral doublets forming the chain of transitions of an odd number of electrodipole transitions. We consider separately cases of rigid and frozen molecules. It is revealed that for the AAS, the configuration structure of the matrix

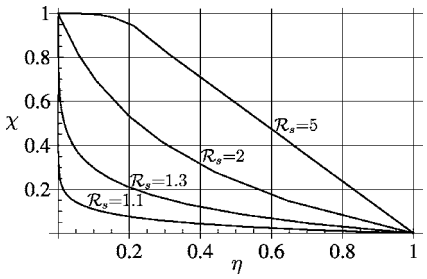

FIG. 9. The degree of chirality χ vs η for various values of the efficiency $\mathcal{R}_s$ of the AAS.

elements of the dipole moments in the chain of transitions must be chiral and a number of obligatory relationships between molecular and field parameters were obtained. Also, we analyzed feasibility of the laser-assisted AAS for the spatially nonlocalized molecules. Derived conditions on the wavevector directions of the laser field components show the ways for constructing the AAS scenarios in a macroscopic active volume with the size significantly exceeding the characteristic wavelengths of the laser fields.

Key results of our analysis are outlined in the set of six conditions for choosing parameters of the laser action, which is the effective tool for construction and analysis of the specific AAS scenarios. The level of generality of the conducted analysis allows us to apply its key results to almost any molecule, to the nonrigid chiral molecules inclusive, at the various regimes of laser action.

For using in the AAS scenarios, we essentially improved the scheme of laser orientation-dependent selection. In the novel scheme, the molecules are selected through modification of the final state of the controlled process with the help of the adiabatic interaction with the three-component coherent laser field and has a number of advantages (elimination of the necessity of using strong electrostatic fields, minimal requirements to molecular properties) in contrast with the scheme suggested by us earlier,[43] which make it essentially more universal and effective.

The general theoretical analysis has been successfully applied to the development of a novel method for laser-assisted AAS from a racemic mixture of noninteractive SiHNaClF molecules. Our calculations show that application of the suggested AAS scheme at room temperature to a macroscopic (with the typical transverse dimensions of about 10 cm) volume of the reagents can give the degree of chirality ~ 0.2 after the photodissociation of the $\frac{4}{5}$ of the initial number of molecules in the active volume. Furthermore, one can expect that the efficiency of the AAS can also be sufficiently improved after additional optimization of the parameters of the laser action. Key destructive contribution to the AAS is due to the parasitic quasiresonant interaction with the excited electronic states.

Discussing further development of the suggested AAS scheme, we must increase its efficacy. One of the perspective directions for that is, in our view, development of the AAS scenarios with more accurate orientation-dependent selection of the molecules due to the use of a larger number of the incident laser field components and due to the excitation of more lengthy chains of photoinduced transitions. Alternatively, one can construct the AAS scenarios, which combine both adiabatic and nonadiabatic methods of laser action based, for instance, on the use of the method of selective population of the dressed states.[54]

ACKNOWLEDGMENTS

We are thankful to Professor Boris Grishanin with whom we had the privilege of collaborating on this and many other problems and who is not with us anymore. We are grateful also to Dr. Julia Vladimirova, Professor Oleg Sarkisov, and Professor Nikolay Zefirov and his co-workers for valuable discussions of the results of this paper.

[1] M. Shapiro and P. Brumer, Rep. Prog. Phys. **66**, 859 (2003).
[2] P. Compain, V. Desvergnes, C. Ollivier, F. Robert, F. Suzenet, M. Barboiu, P. Belmont, Y. Bleriot, F. Bolze, S. Bouquillon, E. Bourguet, B. Braida, T. Constantieux, L. Desaubry, D. Dupont, S. Gastaldi, F. Jerome, S. Legoupy, X. Marat, M. Migaud, N. Moitessier, S. Papot, F. Peri, M. Petit, S. Py, E. Schulz, I. Tranoy-Opalinski, B. Vauzeilles, P. Vayron, L. Vergnes, S. Vidal, and S. Wilmouth, New J. Chem. **30**, 823 (2006).
[3] L. D. Barron, Chem. Soc. Rev. **15**, 189 (1986).
[4] M. Avalos, R. Babiano, P. Cintas, J. L. Jimenez, J. C. Palacios, and L. D. Barron, Chem. Rev. (Washington, D.C.) **98**, 2392 (1998).
[5] J. Shao and P. Hänggi, J. Chem. Phys. **107**, 9935 (1997).
[6] A. Salam and W. J. Meath, Chem. Phys. Lett. **106**, 7865 (1997).
[7] Y. Ma and A. Salam, Chem. Phys. **324**, 367 (2006).
[8] Y. Fujimura, L. Gonzàlez, K. Hoki, J. Manz, and Y. Ohtsuki, Chem. Phys. Lett. **306**, 1 (1999).
[9] L. Gonzàlez, K. Hoki, D. Kröner, A. S. Leal, J. Manz, and Y. Ohtsuki, J. Chem. Phys. **113**, 11134 (2000).
[10] M. Shapiro, E. Frishman, and P. Brumer, Phys. Rev. Lett. **84**, 1669 (2000).
[11] D. Gerbasi, M. Shapiro, and P. Brumer, J. Chem. Phys. **115**, 5349 (2001).
[12] L. Gonzàlez, D. Kröner, and I. R. Sola, J. Chem. Phys. **115**, 2519 (2001).
[13] K. Hoki, Y. Ohtsuki, and Y. Fujimura, J. Chem. Phys. **114**, 1575 (2001).
[14] A. S. Leal, D. Kröner, and L. Gonzàlez, Eur. Phys. J. D **14**, 185 (2001).
[15] K. Hoki, L. Gonzàlez, and Y. Fujimura, J. Chem. Phys. **116**, 2433 (2002).
[16] K. Hoki, L. Gonzàlez, and Y. Fujimura, J. Chem. Phys. **116**, 8799 (2002).
[17] Y. Ohta, K. Hoki, and Y. Fujimura, J. Chem. Phys. **116**, 7509 (2002).
[18] E. Frishman, M. Shapiro, and P. Brumer, J. Phys. B **37**, 2811 (2004).
[19] K. Hoki, D. Kröner, and J. Manz, Chem. Phys. **267**, 59 (2001).
[20] D. Kröner, M. F. Shibl, and L. Gonzàlez, Chem. Phys. Lett. **372**, 242 (2003).
[21] D. Kröner and L. Gonzàlez, Chem. Phys. **298**, 55 (2004).
[22] D. Kröner and L. Gonzàlez, Chem. Phys. **5**, 3933 (2003).
[23] K. Hoki, L. Gonzàlez, M. F. Shibl, and Y. Fujimura, J. Phys. Chem. A **108**, 6455 (2004).
[24] L. Gonzàlez, J. Manz, B. Schmidt, and M. F. Shibl, Phys. Chem. Chem. Phys. **7**, 4096 (2005).
[25] S. S. Bychkov, B. A. Grishanin, and V. N. Zadkov, JETP **116**, 31 (2001).
[26] P. Král and M. Shapiro, Phys. Rev. Lett. **87**, 183002 (2001).
[27] E. Frishman, M. Shapiro, D. Gerbasi, and P. Brumer, J. Chem. Phys. **119**, 7237 (2003).
[28] D. Gerbasi, M. Shapiro, and P. Brumer, J. Chem. Phys. **124**, 074315 (2006).
[29] P. Král, I. Thanopulos, M. Shapiro, and D. Cohen, Phys. Rev. Lett. **90**, 033001 (2003).
[30] I. Thanopulos, P. Král, and M. Shapiro, J. Chem. Phys. **119**, 5105 (2003).
[31] Yu. V. Vladimirova, B. A. Grishanin, D. V. Zhdanov, V. N. Zadkov, and H. Takahashi, Moscow Univ. Phys. Bull. **15**, 1247 (2005).
[32] B. Grishanin, H. Takahashi, Yu. Vladimirova, D. Zhdanov, and V. N. Zadkov, Laser Phys. **15**, 1247 (2005).
[33] N. P. M. Huck, W. F. Jager, B. de Lange, and B. L. Feringa, Science **273**, 1686 (1996).
[34] Y. Shimizu and S. Kawanishi, Chem. Commun. (Cambridge) **1996**, 1333.
[35] Y. Shimizu, J. Chem. Soc., Perkin Trans. 1 **1997**, 1275.
[36] H. Nishino, A. Nakamura, and Y. Inoue, J. Chem. Soc., Perkin Trans. 2 **2001**, 1693; A. Nakamura, H. Nishino, and Y. Inoue, *ibid.* **2001**, 1701; H. Nishino, A. Nakamura, H. Shitomi, H. Onuki, and Y. Inoue, *ibid.* **2001**, 1706.
[37] G. L. J. A. Rikken and E. Raupach, Nature (London) **405**, 932 (2000).
[38] P. Brumer, E. Frishman, and M. Shapiro, Phys. Rev. A **65**, 015401 (2001).
[39] H. Stapelfeldt and T. Seideman, Rev. Mod. Phys. **75**, 543 (2003).
[40] T. Seideman and E. Hamilton, Adv. At., Mol., Opt. Phys. **52**, 289 (2006).
[41] H. Tanji, S. Minemoto, and H. Sakai, Phys. Rev. A **72**, 063401 (2005).
[42] In Refs. 31 and 32, it is shown, for instance, that with reducing initial rotational temperature from zero to 300 K, a relative excess of one enantiomer in the AAS scheme over another is reduced from 14% to $\sim 0.06\%$.
[43] D. V. Zhdanov, B. A. Grishanin, and V. N. Zadkov, JETP **130**, 387 (2006).

[44] From now on, we will assume that the operator $\hat{E}^*$ acts only on molecular coordinates and does not affect the laser field.
[45] Time τ_{tun} varies from a few picosecond up to few million of years, depending on the height of the potential barrier for various chiral molecules. For small τ_{tun}, we have the case of so called dynamical molecular chirality, and for the other limit of the time scale, we have the so called stable chirality.
[46] This stage is also called "enantio discrimination" (Refs. 29 and 30).
[47] P. R. Banker, *Molecular Symmetry and Spectroscopy* (Academic, New York, 1979).
[48] L. D. Landau and E. M. Lifshitz, *Quantum Mechanics. Non-Relativistic Theory* (Pergamon, Oxford, 1991), p. 416.
[49] Let us note that despite the fact that the quantum-mechanical *ab initio* analysis of this molecule shows that it exists and has a bounding electronic term, it would be chemically unstable. Therefore, such a molecule must be considered as a model of prototype molecule for demonstration of the AAS idea rather than for the real experiments.
[50] M. J. Frisch, G. W. Trucks, H. B. Schlegel *et al.*, GAUSSIAN 03, Revision B.05, Gaussian, Inc., Wallingford, CT, 2004.
[51] In these calculations, we used the basis set 6-311G(*d*).
[52] D. Kosloff and R. Kosloff, J. Comput. Phys. **52**, 35 (1983).
[53] M. D. Feit and J. A. Fleck, Jr., J. Chem. Phys. **78**, 301 (1983).
[54] M. Wollenhaupt and T. Baumert, J. Photochem. Photobiol., A **180**, 248 (2006).